Fundamentals of Heat and Mass Transfer

Chapter 7

EXTERNAL FLOW

Dr. Osaid Matar

INTRODUCTION

- Our primary objective is to determine convection coefficients for different flow geometries.

- In particular, we wish to obtain specific forms of the functions that represent these coefficients.

- By **nondimensionalizing the boundary layer equations in Chapter 6, we found that the local and average convection coefficients** may be correlated by equations of the form

Heat Transfer:

$$\mathrm{Nu}_x = f(x^*, \mathrm{Re}_x, \mathrm{Pr})$$

$$\overline{\mathrm{Nu}}_x = f(\mathrm{Re}_x, \mathrm{Pr})$$

INTRODUCTION

- **The experimental or empirical approach involves performing heat transfer measurements under controlled laboratory conditions and correlating the data in terms of appropriate dimensionless parameters**.

- A general discussion of the approach is provided in Section 7.1. It has been applied to many different geometries and flow conditions, and important results are presented in Sections 7.2 through 7.8.

- **The theoretical approach involves solving the boundary layer equations for a particular geometry.**

- For example, **obtaining the temperature profile T*** from such a solution, It may be used to evaluate **the local Nusselt number Nu_x**, and therefore **the local convection coefficient h_x**. With knowledge of how h_x varies over the surface, then it may be used to determine the average convection coefficient , and therefore the average Nusselt number .

The Empirical Method

- The manner in which a convection heat transfer correlation may be obtained experimentally is illustrated in Figure 7.1.

- If a prescribed geometry, such as the flat plate in parallel flow, is heated electrically to maintain $T_s > T_\infty$, convection heat transfer occurs from the surface to the fluid.

- **It would be a simple matter to measure T_s and T_∞, as well as the electrical power, $E \cdot I$, which is equal to the total heat transfer rate q.**

- The convection coefficient , which is an average associated with the entire plate, could then be computed from Newton's law of cooling, **Moreover, from knowledge of the characteristic length L and the fluid properties, the Nusselt, Reynolds, and Prandtl numbers could be computed from their definitions.**

The Empirical Method

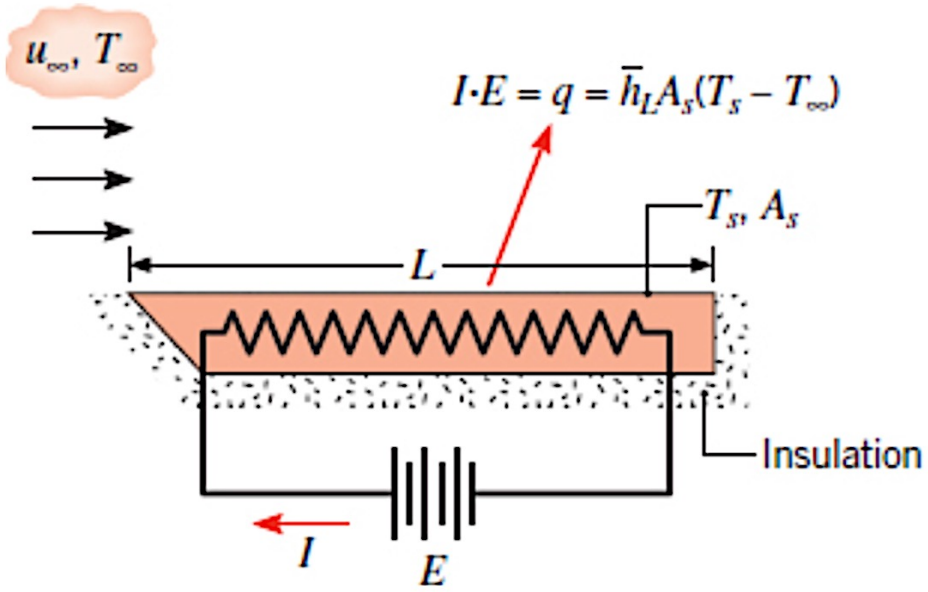

FIGURE 7.1 Experiment for measuring the average convection heat transfer coefficient $\bar{h}_L$.

Copyright ©2017-2019 John Wiley & Sons, Inc.

The Empirical Method

- The foregoing procedure could be repeated for a variety of test conditions. **We could vary the velocity u∞ and the plate length L, as well as the nature of the fluid**, using, for example, **air, water, and engine oil, which have substantially different Prandtl numbers.**

- We would then be left with **many different values of the Nusselt number corresponding to a wide range of Reynolds and Prandtl numbers**, and the results could be plotted on a log–log scale, as shown in Figure 7.2a. Each symbol represents a unique set of test conditions.

- As is often the case, **the results associated with a given fluid, and hence a fixed Prandtl number, fall close to a straight line**, indicating a power law dependence of the Nusselt number on the Reynolds number. **Considering all the fluids**, the data may then be represented by an algebraic expression of the form

$$\bar{\mathrm{Nu}}_L = C\,\mathrm{Re}_L^m\,\mathrm{Pr}^n \qquad \ldots\ldots 7.1$$

The Empirical Method

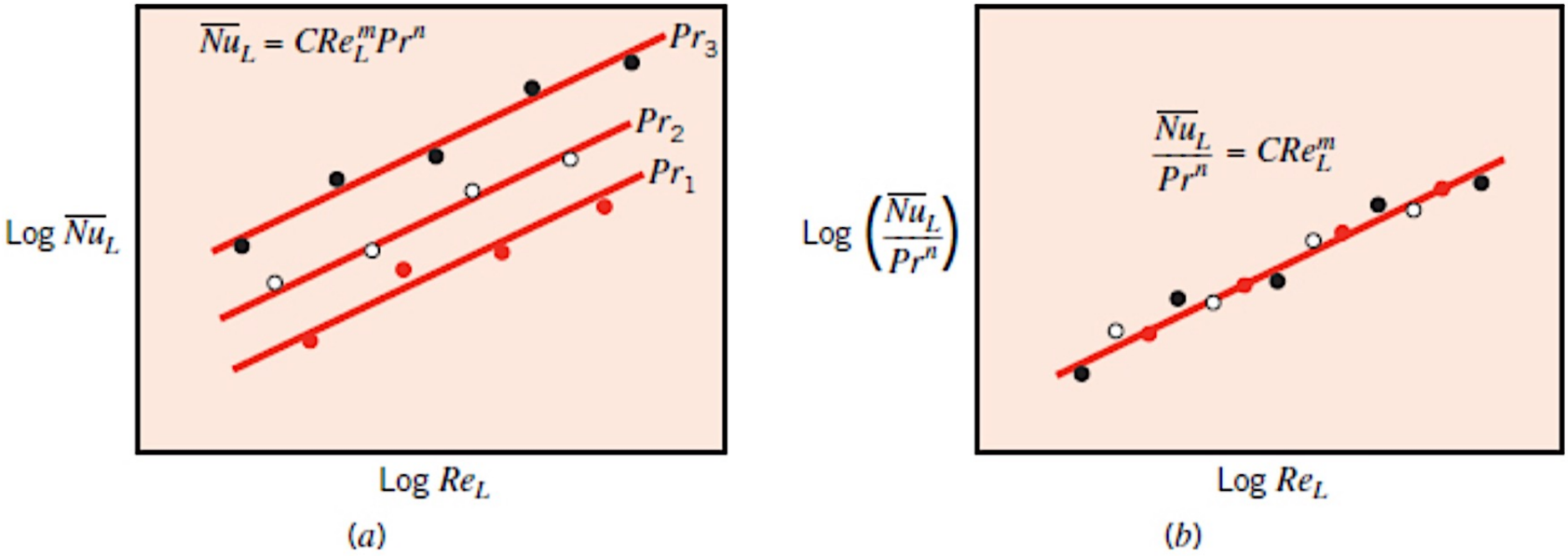

FIGURE 7.2 Dimensionless representation of convection heat transfer measurements.

The Empirical Method

- Since the values of **C, m, and n are often independent of the nature of the fluid**, the family of straight lines corresponding to different Prandtl numbers can be collapsed to a single line by plotting the results in terms of the ratio, as shown in Figure 7.2b.

- Because **Equation 7.1 is inferred from experimental measurements, it is termed an empirical correlation**. **The specific values of the coefficient C and the exponents m and n vary with the nature of the surface geometry and the type of flow.**

- We will use expressions of the form given by Equation 7.1 for many special cases, and it is important to note that the assumption of constant fluid properties is often implicit in the results.

The Empirical Method

- **However, we know that the fluid properties vary with temperature across the boundary layer and that this variation can certainly influence the heat transfer rate.**

- This influence may be handled in one of two ways. In one method, Equation 7.1 is **used with all properties evaluated at a mean boundary layer temperature Tf, termed the film temperature.**

$$T_f \equiv \frac{T_s + T_\infty}{2}$$

- **The alternate method is to evaluate all properties at T∞ and to multiply the right-hand side of Equation 7.1 by an additional parameter to account for the property variations.** The parameter is commonly of the form $(Pr_\infty/Pr_s)^r$ or $(\mu_\infty/\mu_s)^r$, where the subscripts ∞ and s designate evaluation of the properties at the free stream and surface temperatures, respectively. Both methods are used in the results that follow.

The Flat Plate in Parallel Flow

- As discussed before, laminar boundary layer development begins at the leading edge (x = 0) and transition to turbulence may occur at a downstream location (xc) for which a critical Reynolds number Rex,c is achieved.

- **We begin by analytically determining the velocity and temperature, and distributions in the laminar boundary layers that are shown qualitatively in Figures 6.1, 6.2, and 6.3, respectively.**
- **From knowledge of these distributions, we will determine expressions for the local and average friction coefficients and Nusselt numbers.**

- **Subsequently, we will report experimentally determined correlations for the friction coefficient and Nusselt numbers for turbulent boundary layers**.

The Flat Plate in Parallel Flow

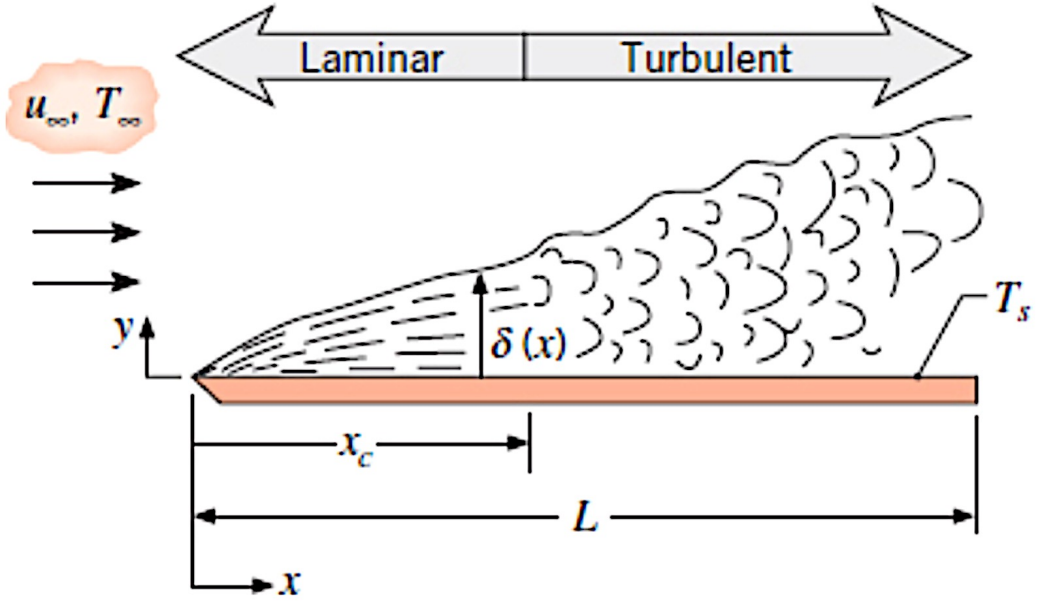

FIGURE 7.3 The flat plate in parallel flow.

Laminar Flow over an Isothermal Plate: A Similarity Solution

- The major convection parameters may be obtained by solving the appropriate form of the boundary layer equations.

- **Assuming steady, incompressible, laminar flow with constant fluid properties and negligible viscous dissipation and recognizing that dp/dx = 0, the boundary layer equations reduce to**

$$\frac{\partial u}{\partial x} + \frac{\partial v}{\partial y} = 0$$ Equations 7.4

$$u\frac{\partial u}{\partial x} + v\frac{\partial u}{\partial y} = \nu\frac{\partial^2 u}{\partial y^2}$$ Equations 7.5

$$u\frac{\partial T}{\partial x} + v\frac{\partial T}{\partial y} = \alpha\frac{\partial^2 T}{\partial y^2}$$ Equations 7.6

The Flat Plate in Parallel Flow

- Solution of these equations is simplified by the fact that for constant properties, **solution of the velocity (hydrodynamic) boundary layer is independent of temperature.**

- **Hence, we may begin by solving the hydrodynamic problem by solving the continuity and momentum equations**

- **Once the hydrodynamic problem has been solved, solutions to the energy equation, which depend on u and υ, may be obtained**.

Hydrodynamic Solution

The hydrodynamic solution follows the method of Blasius [1, 2]. The first step is to define a stream function ψ(x, y), such that

$$u \equiv \frac{\partial \psi}{\partial y} \text{ and } v \equiv -\frac{\partial \psi}{\partial x} \qquad \text{Equations 7.8}$$

Continuity equation is then automatically satisfied and hence is no longer needed.

New dependent and independent variables, f and η, respectively, are then defined such that

$$f(\eta) \equiv \frac{\psi}{u_\infty \sqrt{\nu x / u_\infty}} \qquad \text{Equations 7.9}$$

$$\eta \equiv y \sqrt{u_\infty / \nu x} \qquad \text{Equations 7.10}$$

Hydrodynamic Solution

- As we will find, use of these variables simplifies matters by reducing the partial differential equation, (momentum equation) , to an ordinary differential equation.

- **The Blasius solution is termed a similarity solution, and η is a similarity variable**. This terminology is used because, **despite growth of the boundary layer with distance x from the leading edge, the velocity profile u/u∞ remains geometrically similar.**

- This similarity is of the functional form

$$\frac{u}{u_\infty} = \phi\left(\frac{y}{\delta}\right)$$

where δ is the boundary layer thickness. We will find from the Blasius solution that δ varies as (νx/u∞)1/2; thus, it follows that

$$\frac{u}{u_\infty} = \phi(\eta) \qquad \text{Equations 7.11}$$

Hydrodynamic Solution

$$f(\eta) \equiv \frac{\psi}{u_\infty \sqrt{\nu x / u_\infty}} \qquad \eta \equiv y\sqrt{u_\infty / \nu x}$$

- Hence the velocity profile is uniquely determined by the similarity variable η, which depends on both x and y.
- From Equations 7.8 through 7.10 we obtain

$$u = \frac{\partial \psi}{\partial y} = \frac{\partial \psi}{\partial \eta}\frac{\partial \eta}{\partial y} = u_\infty \sqrt{\frac{\nu x}{u_\infty}}\frac{df}{d\eta}\sqrt{\frac{u_\infty}{\nu x}} = \frac{df}{d\eta} u_\infty \quad \text{Equations 7.12}$$

$$v = -\frac{\partial \psi}{\partial x} = -\left(u_\infty \sqrt{\frac{\nu x}{u_\infty}}\frac{\partial f}{\partial x} + \frac{u_\infty}{2}\sqrt{\frac{\nu}{u_\infty x}} f\right) \quad \text{Equations 7.13}$$

$$v = \frac{1}{2}\sqrt{\frac{\nu u_\infty}{x}}\left(\eta\frac{df}{d\eta} - f\right)$$

By differentiating the velocity components, it may also be shown that

$$\frac{\partial u}{\partial x} = -\frac{u_\infty}{2x}\eta\frac{d^2 f}{d\eta^2} \quad \text{Equations 7.14}$$

Hydrodynamic Solution

$$\frac{\partial u}{\partial y} = u_\infty \sqrt{\frac{u_\infty}{\nu x}} \frac{d^2 f}{d\eta^2}$$ Equations 7.15

$$\frac{\partial^2 u}{\partial y^2} = \frac{u_\infty^2}{\nu x} \frac{d^3 f}{d\eta^3}$$ Equations 7.16

Substituting these expressions into Equation 7.5, we then obtain $u\frac{\partial u}{\partial x} + v\frac{\partial u}{\partial y} = \nu\frac{\partial^2 u}{\partial y^2}$

$$2\frac{d^3 f}{d\eta^3} + f\frac{d^2 f}{d\eta^2} = 0$$ Equations 7.17

Hence the hydrodynamic boundary layer problem is reduced to one of solving a nonlinear, third-order ordinary differential equation. The appropriate boundary conditions are

$$u(x,0) = v(x,0) = 0 \text{ and } u(x,\infty) = u_\infty$$

$$\left.\frac{df}{d\eta}\right|_{\eta=0} = f(0) = 0 \text{ and } \left.\frac{df}{d\eta}\right|_{\eta\to\infty} = 1$$ Equations 7.18

Hydrodynamic Solution

- **The solution subject to the conditions, may be obtained by a series expansion or by numerical integration.**
- Selected results are presented in Table 7.1, from which useful information may be extracted.
- The x-component velocity distribution from the third column of the table is plotted in Figure 7.4a.
- We also note that, to a good approximation, $(u/u\infty) = 0.99$ for $\eta = 5.0$.
- Defining the boundary layer thickness δ as that value of y for which $(u/u\infty) = 0.99$, it follows from Equation 7.10 that

Hydrodynamic Solution

TABLE 7.1 Flat plate laminar boundary layer functions [3]

$\eta = y\sqrt{\frac{u_\infty}{\nu x}}$	f	$\frac{df}{d\eta} = \frac{u}{u_\infty}$	$\frac{d^2 f}{d\eta^2}$
0	0	0	0.332
0.4	0.027	0.133	0.331
0.8	0.106	0.265	0.327
1.2	0.238	0.394	0.317
1.6	0.420	0.517	0.297
2.0	0.650	0.630	0.267
2.4	0.922	0.729	0.228
2.8	1.231	0.812	0.184
3.2	1.569	0.876	0.139
3.6	1.930	0.923	0.098
4.0	2.306	0.956	0.064
4.4	2.692	0.976	0.039
4.8	3.085	0.988	0.022
5.2	3.482	0.994	0.011
5.6	3.880	0.997	0.005
6.0	4.280	0.999	0.002
6.4	4.679	1.000	0.001
6.8	5.079	1.000	0.000

Hydrodynamic Solution

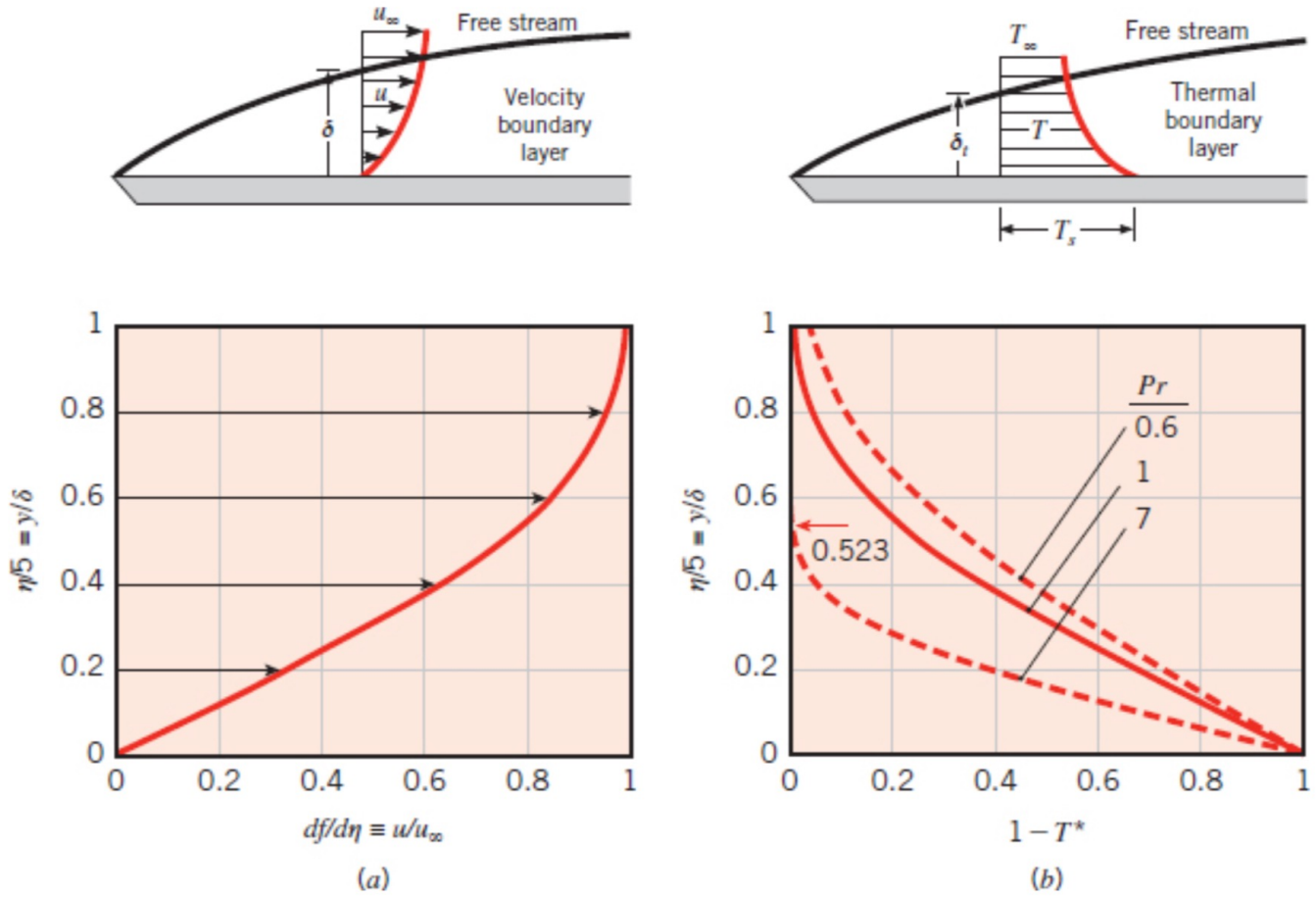

FIGURE 7.4 Similarity solution for laminar flow over an isothermal plate. (a) The x-component of the velocity. (b) Temperature distributions for Pr = 0.6, 1, and 7.

Hydrodynamic Solution

$$\eta \equiv y\sqrt{u_\infty /\nu x}$$

$$\delta = \frac{5.0}{\sqrt{u_\infty /\nu x}} = \frac{5x}{\sqrt{\mathrm{Re}_x}}$$

Equation 7.19

From Equation 7.19 it is clear that δ increases with increasing x and ν but decreases with increasing u∞ **(the larger the free stream velocity, the thinner the boundary layer)**. In addition, from Equation 7.15 the wall shear stress may be expressed as

$$\tau_s = \mu\frac{\partial \mathrm{u}}{\partial \mathrm{y}}\bigg|_{y=0} = \mu u_\infty \sqrt{u_\infty /\nu x}\frac{d^2 f}{d\eta^2}\bigg|_{\eta=0}$$

$$\tau_s = 0.332 u_\infty \sqrt{\rho\mu u_\infty /x}$$

$$C_{f,x} \equiv \frac{\tau_{s,x}}{\rho u_\infty^2 /2} = 0.664\,\mathrm{Re}_x^{-1/2}$$

Equation 7.20

Heat Transfer Solution

From knowledge of conditions in the velocity boundary layer, the energy equation may now be solved. We begin by introducing the dimensionless temperature $T^* \equiv [(T - T_s)/(T_\infty - T_s)]$ and assume a similarity solution of the form $T^* = T^*(\eta)$. Making the necessary substitutions, Equation 7.6 reduces to

$$\frac{d^2 T^*}{d\eta^2} + \frac{\Pr}{2} f \frac{dT^*}{d\eta} = 0 \qquad \text{Equation 7.21}$$

Note the dependence of the thermal solution on hydrodynamic conditions through appearance of the variable f in Equation 7.21. The appropriate boundary conditions are

$$T^*(0) = 0 \text{ and } T^*(\infty) = 1 \qquad \text{Equation 7.22}$$

Heat Transfer Solution

- Subject to the conditions of Equation 7.22, Equation 7.21 may be solved by numerical integration for different values of the Prandtl number; representative temperature distributions for Pr = 0.6, 1, and 7 are shown in Figure 7.4b.

- **The temperature distribution is identical to the velocity distribution for Pr = 1.**

- Thermal effects penetrate farther into the velocity boundary layer with decreasing Prandtl number and transcend the velocity boundary layer for Pr < 1.

- **A practical consequence of this solution is that, for Pr $\gtrsim$ 0.6, results for the surface temperature gradient $dT^*/d\eta|_{\eta=0}$ may be correlated by the following relation:**

$$\left.\frac{dT^*}{d\eta}\right|_{\eta=0} = 0.332\,\mathrm{Pr}^{1/3}$$

Heat Transfer Solution

- Expressing the local convection coefficient as

$$h_x = \frac{q_s''}{T_s - T_\infty} = -\frac{T_\infty - T_s}{T_s - T_\infty} k \frac{\partial T^*}{\partial y}\bigg|_{y=0}$$

$$h_x = k\left(\frac{u_\infty}{\nu x}\right)^{1/2} \frac{dT^*}{d\eta}\bigg|_{\eta=0}$$

it follows that the local Nusselt number is

$$\mathrm{Nu}_x \equiv \frac{h_x x}{k} = 0.332\,\mathrm{Re}_x^{1/2}\,\mathrm{Pr}^{1/3} \quad \mathrm{Pr} \gtrsim 0.6$$ Equation 7.23

Heat Transfer Solution

From the solution to Equation 7.21, it also follows that, for Pr $\gtrsim$ 0.6, the ratio of the velocity to thermal boundary layer thickness is

$$\frac{d^2 T^*}{d\eta^2} + \frac{\Pr}{2} f \frac{dT^*}{d\eta} = 0$$

$$\frac{\delta}{\delta_t} \approx \Pr^{1/3}$$

Equation 7.24

Average Boundary Layer Parameters for Laminar Conditions

From the foregoing local results, average boundary layer parameters may be determined. With the average friction coefficient defined as

$$\bar{C}_{f,x} \equiv \frac{\bar{\tau}_{s,x}}{\rho u_\infty^2/2}$$

$$\bar{\tau}_{s,x} \equiv \frac{1}{x}\int_0^x \tau_{s,x}\, dx$$

$$\bar{C}_{f,x} = 1.328\, Re_x^{-1/2}$$

$$\bar{h}_x = \frac{1}{x}\int_0^x h_x\, dx = 0.332\left(\frac{k}{x}\right)Pr^{1/3}\left(\frac{u_\infty}{\nu}\right)^{1/2}\int_0^x \frac{dx}{x^{1/2}}$$

$$Nu_x \equiv \frac{h_x x}{k} = 0.332\, Re_x^{1/2}\, Pr^{1/3} \quad Pr \gtrsim 0.6$$

Integrating and substituting from Equation 7.23, it follows that $\bar{h}_x = 2h_x$. Hence

$$Nu_x \equiv \frac{\bar{h}_x x}{k} = 0.664\, Re_x^{1/2}\, Pr^{1/3} \quad Pr \gtrsim 0.6$$

Liquid Metals

For fluids of small Prandtl number, namely, liquid metals, Equation 7.23 does not apply.

However, for this case the thermal boundary layer development is much more rapid than that of the velocity boundary layer
($\delta t \gg \delta$), and it is reasonable to assume uniform velocity ($u = u\infty$) throughout the thermal boundary layer.

From a solution to the thermal boundary layer equation based on this assumption [5], it may then be shown that

$$Nu_x = 0.564\, Pe_x^{1/2} \quad Pr \lesssim 0.05, \quad Pe_x \gtrsim 100$$

NOTE: For liquid metals, the Prandtl number is typically very low compared to other fluids like water or air. This is because liquid metals generally **have high thermal conductivity and low viscosity.**

where $Pe_x \equiv Re_x\ Pr$ is the Peclet number (Table 6.2). **Despite the corrosive and reactive nature of liquid metals, their unique properties (low melting point and vapor pressure, as well as high thermal capacity and conductivity) render them attractive as coolants in applications requiring high heat transfer rates.**

Peclet number (Pe_L)	$\frac{VL}{\alpha} = Re_L\ Pr$	Ratio of advection to conduction heat transfer rates

A single correlating equation, which applies for all Prandtl numbers, has been recommended by Churchill and Ozoe [6]. For laminar flow over an isothermal plate, the local convection coefficient may be obtained from

$$\overline{Nu}_x = \frac{0.3387\ Re_x^{1/2}\ Pr^{1/3}}{[1 + (0.0468/Pr)^{2/3}]^{1/4}}\ Pe_x \gtrsim 100$$

with $\overline{Nu}_x = 2Nu_x$.

Turbulent Flow over an Isothermal Plate

It is not possible to obtain exact analytical solutions for turbulent boundary layers, which are inherently unsteady. From experiment [2] it is known that, for turbulent flows with Reynolds numbers up to approximately 10^8, the local friction coefficient is correlated to within 15% accuracy by an expression of the form

$$C_{f,x} = 0.0592\,\mathrm{Re}_x^{-1/5} \quad \mathrm{Re}_{x,c} \lesssim \mathrm{Re}_x \lesssim 10^8$$

$$\delta = 0.37x\,\mathrm{Re}_x^{-1/5}$$

Using Equation 7.34 with the modified Reynolds, or Chilton–Colburn, analogy, the local Nusselt number for turbulent flow is

$$\mathrm{Nu}_x = \mathrm{St}\,\mathrm{Re}_x\,\mathrm{Pr} = 0.0296\,\mathrm{Re}_x^{4/5}\,\mathrm{Pr}^{1/3} \quad 0.6 \lesssim \mathrm{Pr} \lesssim 60$$

Unheated Starting Length

All the foregoing Nusselt number expressions are restricted to situations for which the surface temperature Ts is uniform. A common exception involves existence of an unheated starting length (Ts = T∞) upstream of a heated section (Ts ≠ T∞). As shown in Figure 7.5, velocity boundary layer growth begins at x = 0, while thermal boundary layer development begins at x = ξ. Hence there is no heat transfer for $0 \leq x \leq \xi$. Through use of an integral boundary layer solution [5], it is known that, for laminar flow

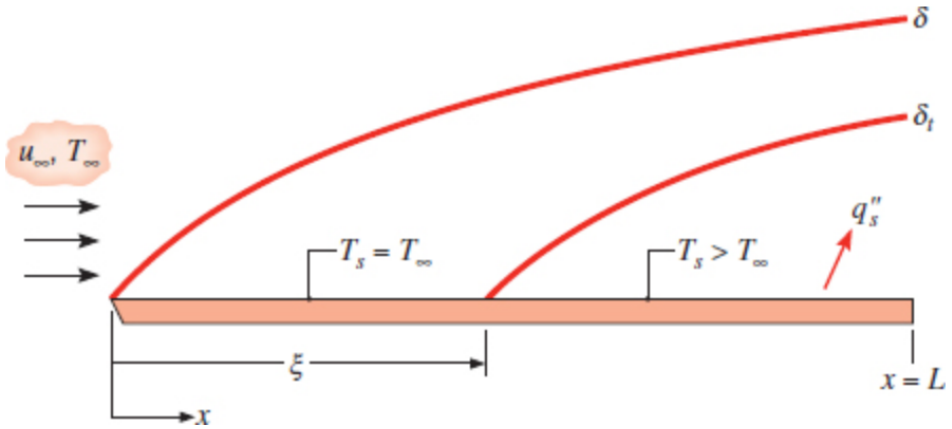

FIGURE 7.5 Flat plate in parallel flow with unheated starting length.

$$\mathrm{Nu}_x = \frac{\mathrm{Nu}_x|_{\xi=0}}{[1-(\xi/x)^{3/4}]^{1/3}}$$

It has also been found that, for turbulent flow,

$$\mathrm{Nu}_x = \frac{\mathrm{Nu}_x|_{\xi=0}}{[1-(\xi/x)^{9/10}]^{1/9}}$$

For a plate of total length L, with laminar or turbulent flow over the entire surface, the expressions are of the form

(7.44)

$$\mathrm{Nu}_L = \mathrm{Nu}_L\Big|_{\xi=0} \frac{L}{L-\xi}[1-(\xi/L)^{(p+1)/(p+2)}]^{p/(p+1)}$$

where p = 2 for laminar flow and p = 8 for turbulent flow.

Flat Plates with Constant Heat Flux Conditions

It is also possible to have a uniform surface heat flux, rather than a uniform temperature, imposed at the plate. For laminar flow, it may be shown that [5]

$$\mathrm{Nu}_x = 0.0308\,\mathrm{Re}_x^{4/5}\,\mathrm{Pr}^{1/3} \quad 0.6 \lesssim \mathrm{Pr} \lesssim 60$$

$$T_s(x) = T_\infty + \frac{q_s''}{h_x}$$

An average surface temperature $(T_s - \bar{T}_\infty) = \frac{1}{L}\int_0^L (T_s - T_\infty)\mathrm{dx} = \frac{q_s''}{L}\int_0^L \frac{x}{k\mathrm{Nu}_x}\mathrm{dx}$

$$(T_s - \bar{T}_\infty) = \frac{q_s'' L}{k\mathrm{Nu}_L}$$

Where:

$$\mathrm{Nu}_L = 0.680\,\mathrm{Re}_L^{1/2}\,\mathrm{Pr}^{1/3}$$

IHT Example 7.1

Air at a pressure of 6 kN/m^2 and a temperature of 300°C flows with a velocity of 10 m/s over a flat plate 0.5 m long. Estimate the cooling rate per unit width of the plate needed to maintain it at a surface temperature of 27°C.

Solution

Known: Airflow over an isothermal flat plate.

Find: Cooling rate per unit width of the plate, q' (W/m).

Schematic:

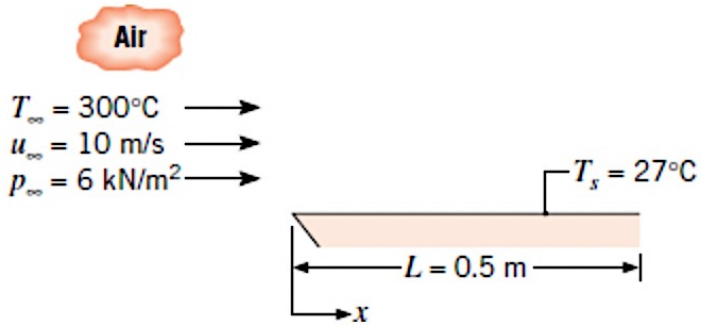

Assumptions:

1. Steady-state, incompressible flow conditions.

2. Negligible radiation effects.

Properties: Table A.4, air (T_f = 437 K, p = 1 atm): $\nu = 30.84 \times 10^{-6}$ m^2/s, $k = 36.4 \times 10^{-3}$ W/m · K, Pr = 0.687. As noted in Example 6.6, the properties k, Pr, c_p, and μ may be assumed to be independent of pressure. However, for an ideal gas, the kinematic viscosity is inversely proportional to pressure. Hence the kinematic viscosity of air at 437 K and $p_\infty = 6 \times 10^3$ N/m^2 is

$$\nu = 30.84 \times 10^{-6}\ \text{m}^2/\text{s} \times \frac{1.0133 \times 10^5\ \text{N/m}^2}{6 \times 10^3\ \text{N/m}^2} = 5.21 \times 10^{-4}\ \text{m}^2/\text{s}$$

Analysis: For a plate of unit width, it follows from Newton's law of cooling that the rate of convection heat transfer *to* the plate is

$$q' = \bar{h} L (T_\infty - T_s)$$

To determine the appropriate convection correlation for computing $\bar{h}$, the Reynolds number must first be determined

$$\text{Re}_L = \frac{u_\infty L}{\nu} = \frac{10\ \text{m/s} \times 0.5\ \text{m}}{5.21 \times 10^{-4}\ \text{m}^2/\text{s}} = 9597$$

Hence the flow is laminar over the entire plate, and the appropriate correlation is given by Equation 7.30.

$$\overline{\text{Nu}}_L = 0.664\ \text{Re}_L^{1/2}\ \text{Pr}^{1/3} = 0.664(9597)^{1/2}(0.687)^{1/3} = 57.4$$

The average convection coefficient is then

$$\bar{h} = \frac{\overline{\text{Nu}}_L k}{L} = \frac{57.4 \times 0.0364\ \text{W/m} \cdot \text{K}}{0.5\ \text{m}} = 4.18\ \text{W/m}^2 \cdot \text{K}$$

and the required cooling rate per unit width of plate is

$$q' = 4.18\ \text{W/m}^2 \cdot \text{K} \times 0.5\ \text{m}\ (300 - 27)^\circ\text{C} = 570\ \text{W/m} \qquad \triangleleft$$

Comments:

1. The results of Table A.4 apply to gases at atmospheric pressure.

2. Example 7.1 in *IHT* demonstrates how to use the *Correlations* and *Properties* tools, which can facilitate performing convection calculations.

EXAMPLE 7.2

A flat plate of width $w = 1$ m is maintained at a uniform surface temperature of $T_s = 230°C$ by using independently controlled heated segments, each of which is $L_h = 50$ mm long. If atmospheric air at 25°C flows over the plate at a velocity of 60 m/s, which segment requires the largest heater power, and what is the value of this power?

SOLUTION

Known: Airflow over a flat plate with segmented heaters.

Find: Maximum heater power requirement.

Schematic:

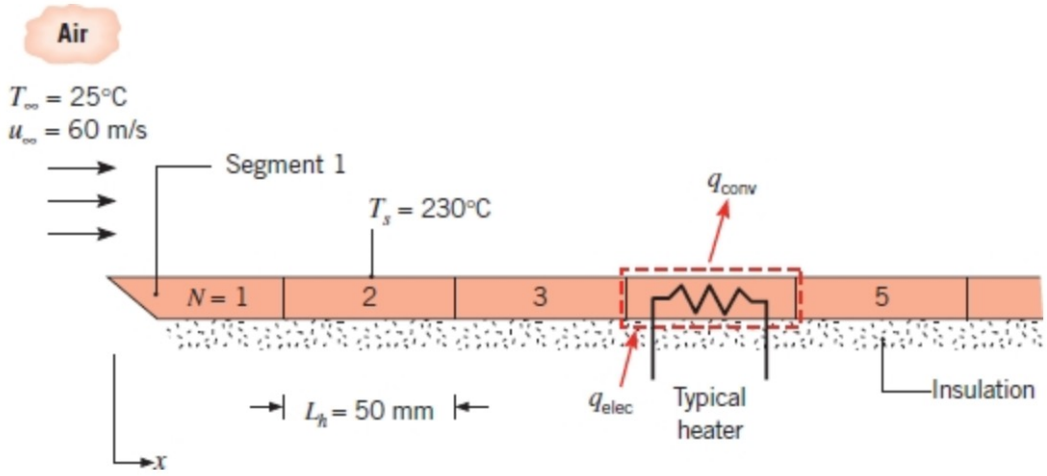

Assumptions:

1. Steady-state, incompressible flow conditions.

2. Negligible radiation effects.

3. Bottom surfaces of heated segments are adiabatic.

Properties: Table A.4, air ($T_f = 400$ K, $p = 1$ atm): $\nu = 26.41 \times 10^{-6}$ m^2/s, $k = 0.0338$ W/m · K, $Pr = 0.690$.

Analysis: The Reynolds number based upon the length, L_h of the first heated segment is

$$\mathrm{Re}_1 = \frac{u_\infty L_h}{\nu} = \frac{60\ \mathrm{m/s} \times 0.05\ \mathrm{m}}{26.41 \times 10^{-6}\ \mathrm{m^2/s}} = 1.14 \times 10^5$$

If the transition Reynolds number is assumed to be $Re_{x,c} = 5 \times 10^5$, it follows that transition will occur at

$$x_c = \frac{\nu}{u_\infty}\mathrm{Re}_{x,c} = \frac{26.41 \times 10^{-6}\ \mathrm{m^2/s}}{60\ \mathrm{m/s}} 5 \times 10^5 = 0.22\ \mathrm{m}$$

which is within the fifth heated segment. Knowing how the local convection coefficient varies with distance from the leading edge of the plate, there are three possibilities regarding which segment will have the maximum power requirement:

1. Segment 1, since it corresponds to the largest local, laminar convection coefficient.

2. Segment 5, since it corresponds to the largest local, turbulent convection coefficient.

3. Segment 6, since turbulent conditions exist over the entire segment.

In general, for heater segment N, the power requirement is

$$q_{\mathrm{elec},N} = q_{\mathrm{conv},N} = \bar{h}_N L_h\ w(T_s - T_\infty) \tag{1}$$

Applying the conservation of energy principle, the power requirement for segment N may be determined by subtracting the rate of heat loss associated with the first $N-1$ segments from the rate of heat loss associated with all N segments. With $\bar{h}_{1-N}$ defined as the average convection heat transfer coefficient over segments 1 through N, the power requirement for segment N is equal to the rate of convection heat transfer from the segment, which may be expressed as

$$\begin{aligned} q_{\mathrm{conv},N} &= \bar{h}_{1-N}(NL_h)w(T_s - T_\infty) - \bar{h}_{1-(N-1)}[(N-1)L_h]w(T_s - T_\infty) \\ &= [N\bar{h}_{1-N} - (N-1)\bar{h}_{1-(N-1)}]L_h\, w(T_s - T_\infty) \end{aligned} \tag{2}$$

Combining Equations 1 and 2 yields

$$\bar{h}_N = N\bar{h}_{1-N} - (N-1)h_{1-(N-1)} \tag{3}$$

Segment 1: The flow is laminar, and the average convection coefficient, $\bar{h}_1$, may be determined from Equation 7.30,

$$Nu_1 = 0.664\,\mathrm{Re}_1^{1/2}\,\mathrm{Pr}^{1/3} = 0.664(1.14\times10^5)^{1/2}(0.69)^{1/3} = 198$$

yielding

$$\bar{h}_1 = \frac{Nu_1\,k}{L_h} = \frac{198\times0.0338\ \mathrm{W/m\cdot K}}{0.05\ \mathrm{m}} = 134\ \mathrm{W/m^2\cdot K}$$

Segment 5: Mixed conditions exist. The average Nusselt number for segments 1 through 5 may be obtained from Equation 7.38 with $A = 871$ and $Re_5 = 5Re_1 = 5.68\times10^5$:

$$Nu_5 = (0.037\,\mathrm{Re}_5^{4/5} - 871)\mathrm{Pr}^{1/3} = [0.037(5.68\times10^5)^{4/5} - 871](0.69)^{1/3} = 542$$

Therefore

$$\bar{h}_{1-5} = \frac{Nu_5\,k}{5L_h} = \frac{542\times0.0338\ \mathrm{W/m\cdot K}}{0.25\ \mathrm{m}} = 73.3\ \mathrm{W/m^2\cdot K}$$

The value of Nu_4 may be obtained from Equation 7.30. With $Re_4 = 4Re_1 = 4.54\times10^5$,

$$Nu_4 = 0.664(4.54\times10^5)^{1/2}(0.69)^{1/3} = 396$$

Therefore

$$\bar{h}_{1-4} = \frac{Nu_4\,k}{4L_h} = \frac{396\times0.0338\ \mathrm{W/m\cdot K}}{0.2\ \mathrm{m}} = 66.8\ \mathrm{W/m^2\cdot K}$$

Evaluation of Equation 3 yields

$$\bar{h}_5 = 5\bar{h}_{1-5} - 4\bar{h}_{1-4} = 5 \times 73.3\ \text{W/m}^2 \cdot \text{K} - 4 \times 66.8\ \text{W/m}^2 \cdot \text{K} = 99.3\ \text{W/m}^2 \cdot \text{K}$$

Segment 6: The value of Nu_6 may be obtained from Equation 7.38. With $Re_6 = 6Re_1 = 6.84 \times 10^5$,

$$Nu_6 = [0.037(6.82 \times 10^5)^{4/5} - 871](0.69)^{1/3} = 748$$

Therefore

$$\bar{h}_{1-6} = \frac{Nu_6\, k}{6L_h} = \frac{748 \times 0.0338\ \text{W/m} \cdot \text{K}}{0.3\ \text{m}} = 84.3\ \text{W/m}^2 \cdot \text{K}$$

Equation 3 yields

$$\bar{h}_6 = 6\bar{h}_{1-6} - 5\bar{h}_{1-5} = 6 \times 84.3\ \text{W/m}^2 \cdot \text{K} - 5 \times 73.3\ \text{W/m}^2 \cdot \text{K} = 139\ \text{W/m}^2 \cdot \text{K}$$

Since $\bar{h}_6 > \bar{h}_1 > \bar{h}_5$, the maximum power requirement is associated with segment 6 and is

$$q_{\text{conv},6} = \bar{h}_6\, L_h\, w(T_s - T_\infty) = 139\ \text{W/m}^2 \cdot \text{K} \times 0.05\ \text{m} \times 1\ \text{m} \times (230°\text{C} - 25°\text{C}) = 1430\ \text{W}$$

Comments:

1. A less accurate, alternative approach is to assume that the average heat transfer coefficient for a particular segment N is well represented by the value of the local heat transfer coefficient at the middle of the segment, $x_{\text{mid},N}$. The following results were obtained using this approach.

Segment	$x_{\text{mid},N}$ **(m)**	**Flow**	**Correlation**	$h_{x,\text{mid}}$ **(W/m² · K)**
1	0.025	Laminar	Equation 7.23	$95 \neq \bar{h}_1$
5	0.225	Turbulent	Equation 7.36	$145 \neq \bar{h}_5$
6	0.275	Turbulent	Equation 7.36	$139 \approx \bar{h}_6$

With this approach, we not only predict incorrect values of the average heat transfer coefficient for each segment, but we also incorrectly identify segment 5 as having the largest power requirement. This procedure yields reasonable results only when spatial variation of the convection coefficient is gradual, such as in regions of turbulent flow that are not in the vicinity of the flow transition.

The Cylinder in Cross Flow

Another common external flow involves fluid motion normal to the axis of a circular cylinder.

As shown in Figure 7.6, the free stream fluid is brought to rest at the forward stagnation point, with an accompanying rise in pressure.

From this point, the pressure decreases with increasing x, the streamline coordinate, and the boundary layer develops under the influence of a favorable pressure gradient ($dp/dx < 0$).

However, the pressure must eventually reach a minimum, and toward the rear of the cylinder further boundary layer development occurs in the presence of an adverse pressure gradient ($dp/dx > 0$).

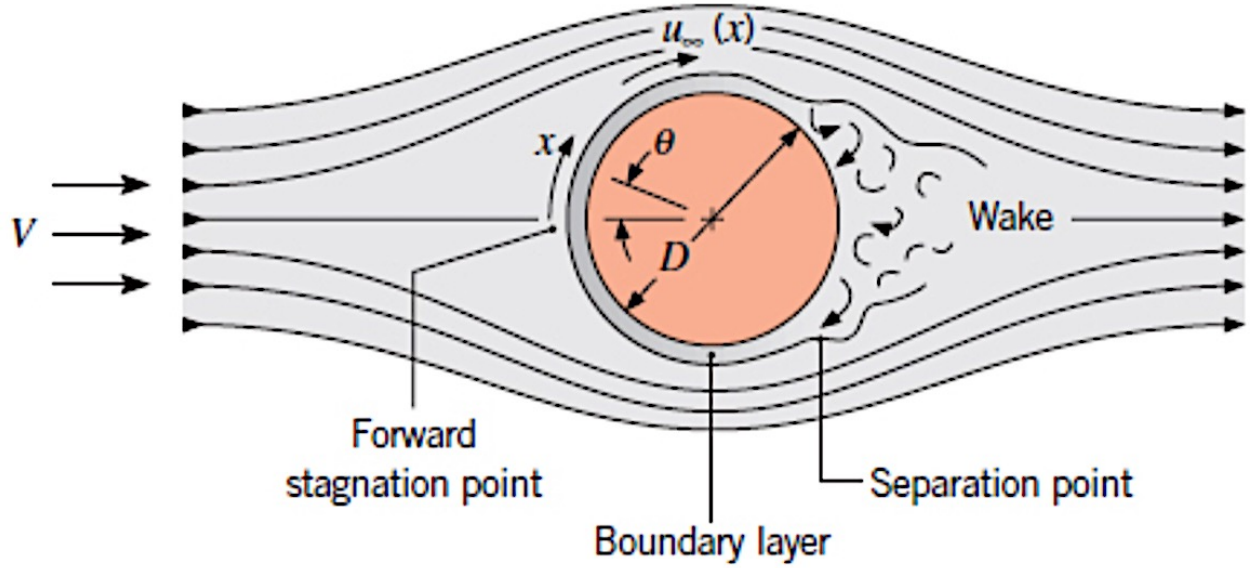

FIGURE 7.6 Boundary layer formation and separation on a circular cylinder in cross flow.

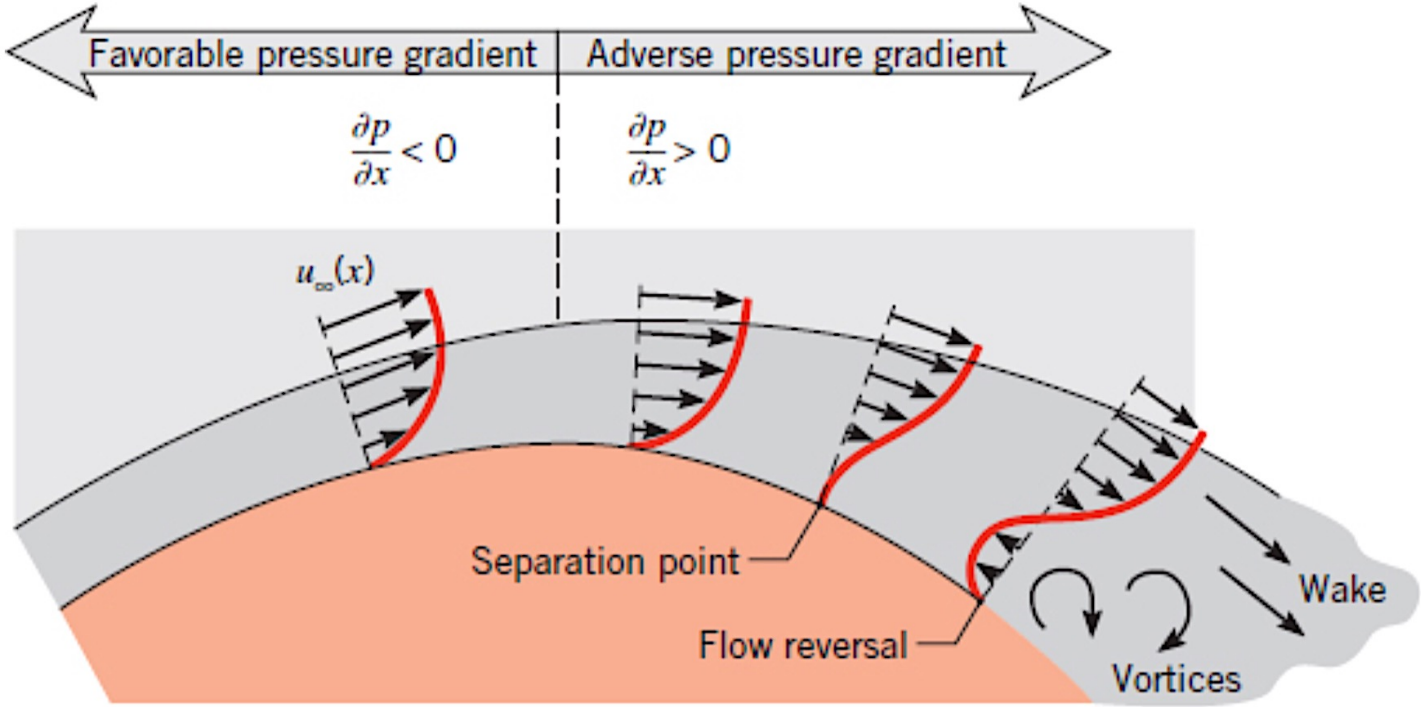

FIGURE 7.7 Velocity profile associated with separation on a circular cylinder in cross flow

In Figure 7.6, the distinction between the upstream velocity V and the free stream velocity u_∞ should be noted.

Unlike conditions for the flat plate in parallel flow, these velocities differ, with u_∞ now depending on the distance x from the stagnation point.

From Euler's equation for an inviscid flow [10], $u_\infty(x)$ must exhibit behavior opposite to that of p(x).

That is, from $u_\infty = 0$ at the stagnation point, the fluid accelerates because of the favorable pressure gradient ($du_\infty/dx > 0$ when $dp/dx < 0$), reaches a maximum velocity when $dp/dx = 0$, and decelerates because of the adverse pressure gradient ($du_\infty/dx < 0$ when $dp/dx > 0$).

As the fluid decelerates, the velocity gradient at the surface, $\partial u/\partial y|y = 0$, eventually becomes zero (Figure 7.7).

At this location, termed the separation point, fluid near the surface lacks sufficient momentum to overcome the pressure gradient, and continued downstream movement is impossible.

Since the oncoming fluid also precludes flow back upstream, boundary layer separation must occur.

This is a condition for which the boundary layer detaches from the surface, and a wake is formed in the downstream region.

Flow in this region is characterized by vortex formation and is highly irregular.

The occurrence of boundary layer transition, which depends on the Reynolds number, strongly influences the position of the separation point. For the circular cylinder the characteristic length is the diameter, and the Reynolds number is defined as

Since the momentum of fluid in a turbulent boundary layer is larger than in the laminar boundary layer, it is reasonable to expect transition to delay the occurrence of separation. If $Re_D \lesssim 2 \times 10^5$, the boundary layer is laminar, and separation occurs at $\theta \approx 80°$ (Figure 7.8). However, if $Re_D \gtrsim 2 \times 10^5$, boundary layer transition occurs, and separation is delayed to $\theta \approx 140°$.

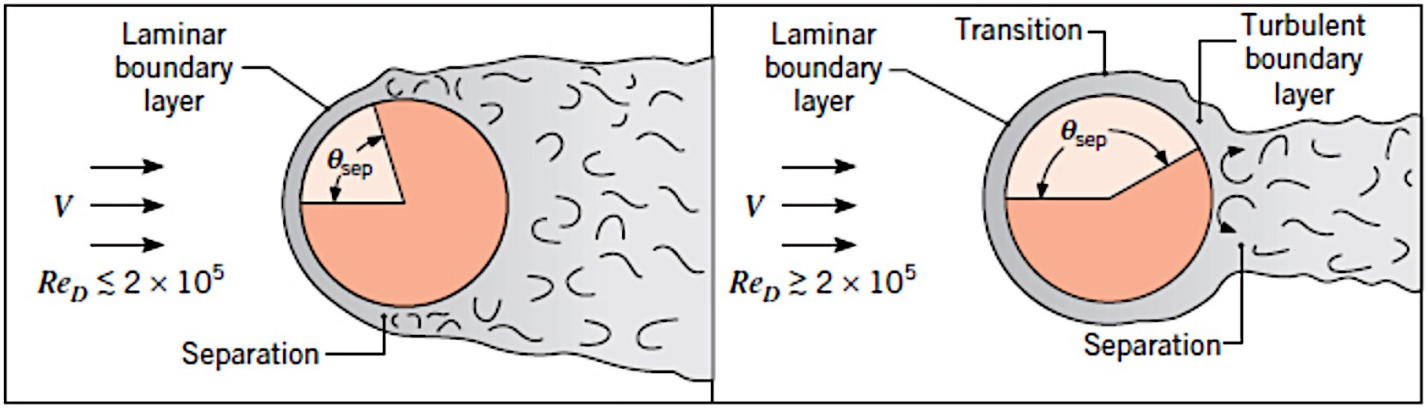

FIGURE 7.8 The effect of turbulence on separation.

The foregoing processes strongly influence the drag force, FD, acting on the cylinder.

This force has two components, one of which is due to the boundary layer surface shear stress (friction drag).

The other component is due to a pressure differential in the flow direction resulting from formation of the wake (form, or pressure, drag).

A dimensionless drag coefficient CD may be defined as

$$C_D \equiv \frac{F_D}{A_f(\rho V^2/2)}$$

where A_f is the cylinder frontal area (the area projected perpendicular to the free stream velocity).

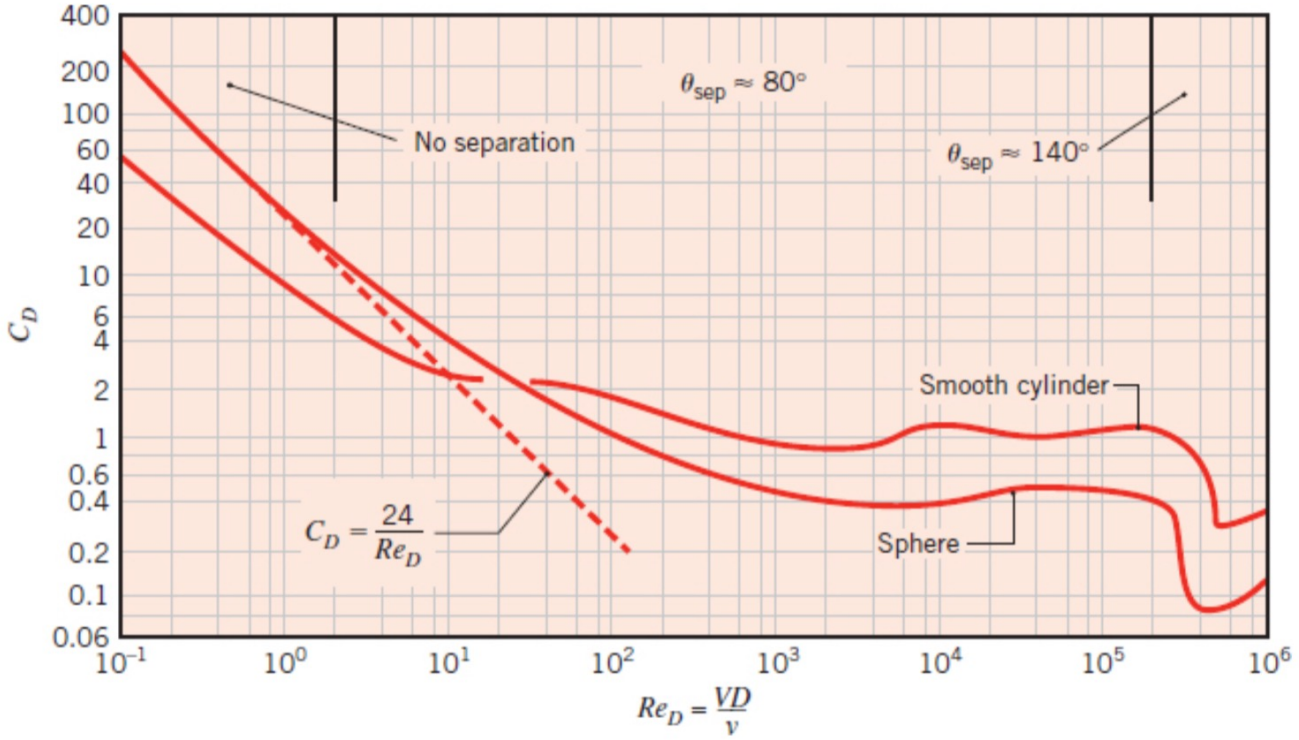

FIGURE 7.9 Drag coefficients for a smooth circular cylinder in cross flow and for a sphere. Boundary layer separation angles are for a cylinder. Based on Schlichting, H., and K. Gersten, *Boundary Layer Theory*, Springer, New York, 2000.

Convection Heat

An empirical correlation due to Hilpert [12] that has been modified to account for fluids of various Prandtl numbers,

$$\mathrm{Nu}_D \equiv \frac{\bar{h}D}{k} = C\,\mathrm{Re}_D^m\,\mathrm{Pr}^{1/3}$$

is widely used for Pr $\gtrsim$ 0.7,

All properties are evaluated at the film temperature.

TABLE 7.2 Constants of Equation 7.52 for the circular cylinder in cross flow [12, 13]

Re_D	C	m
0.4–4	0.989	0.330
4–40	0.911	0.385
40–4000	0.683	0.466
4000–40,000	0.193	0.618
40,000–400,000	0.027	0.805

TABLE 7.3 Constants of Equation 7.52 for noncircular cylinders in cross flow of a gas [14, 15][a]

Geometry	Re_D	C	m
Square 	6000–60,000	0.304	0.59
	5000–60,000	0.158	0.66
Hexagon 	5200–20,400 20,400–105,000	0.164 0.039	0.638 0.78
	4500–90,700	0.150	0.638
Thin plate perpendicular to flow 	10,000–50,000 7000–80,000	0.667 0.191	0.500 0.667

Other correlations have been suggested for the circular cylinder in cross flow [16, 17, 18]. The correlation due to Zukauskas [17] is of the form

$$\mathrm{Nu}_D = C\,\mathrm{Re}_D^m\,\mathrm{Pr}^n\left(\frac{\mathrm{Pr}}{\mathrm{Pr}_s}\right)^{1/4}$$

$$\left[\begin{array}{l} 0.7 \lesssim \mathrm{Pr} \lesssim 500 \\ 1 \lesssim \mathrm{Re}_D \lesssim 10^6 \end{array}\right]$$

TABLE 7.4 Constants of Equation 7.53 for the circular cylinder in cross flow [18]

Re_D	C	m
1–40	0.75	0.4
40–1000	0.51	0.5
10^3–2×10^5	0.26	0.6
2×10^5–10^6	0.076	0.7

where all properties are evaluated at T∞, except Prs, which is evaluated at Ts.

Values of C and m are listed in Table 7.4. If Pr ≲ 10, n = 0.37; if Pr ≳ 10, n = 0.36.

Churchill and Bernstein [18] have proposed a single comprehensive equation that covers the entire range of ReD for which data are available, as well as a wide range of Pr. The equation is recommended for all Re_D Pr $\gtrsim$ 0.2 and has the form

$$\overline{Nu}_D = 0.3 + \frac{0.62\,Re_D^{1/2}\,Pr^{1/3}}{[1+(0.4/Pr)^{2/3}]^{1/4}}\left[1+\left(\frac{Re_D}{282{,}000}\right)^{5/8}\right]^{4/5}$$

EXAMPLE 7.4

Experiments have been conducted using a metallic cylinder 12.7 mm in diameter and 94 mm long. The cylinder is heated internally by an electrical heater and is subjected to a cross flow of air in a low-speed wind tunnel. Under a specific set of operating conditions for which the upstream air velocity and temperature were maintained at V = 10 m/s and 26.2°C, respectively, the heater power dissipation was measured to be P = 46 W, while the average cylinder surface temperature was determined to be Ts = 128.4°C.

It is estimated that 15% of the power dissipation is lost through the cumulative effects of surface radiation and conduction through the endpieces. The cumulative uncertainty associated with (i) the air velocity and temperature measurements, (ii) estimating the heat losses by radiation and from the cylinder ends, and (iii) averaging the cylinder surface temperature, which varies axially and circumferentially, renders the experimental value of the convection coefficient accurate to no better than 20%.

1. Determine the convection heat transfer coefficient from the experimental observations.
2. Compare the experimental result with the convection coefficient computed from an appropriate correlation.

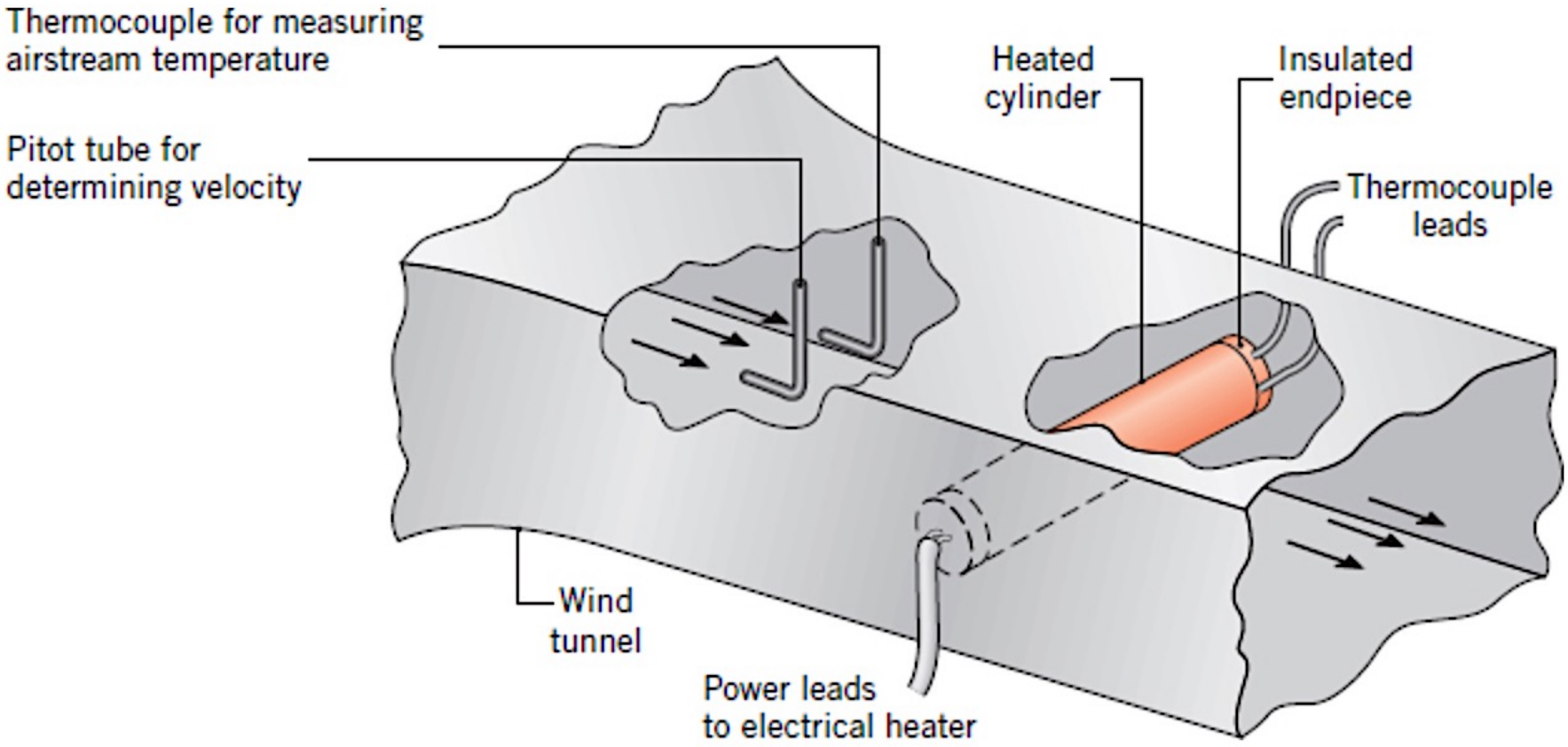
Thermocouple for measuring airstream temperature
Pitot tube for determining velocity
Heated cylinder
Insulated endpiece
Thermocouple leads
Wind tunnel
Power leads to electrical heater

SOLUTION

Known: Operating conditions for a heated cylinder.
Find:

1. Convection coefficient associated with the operating conditions.
2. Convection coefficient from an appropriate correlation.

Schematic:

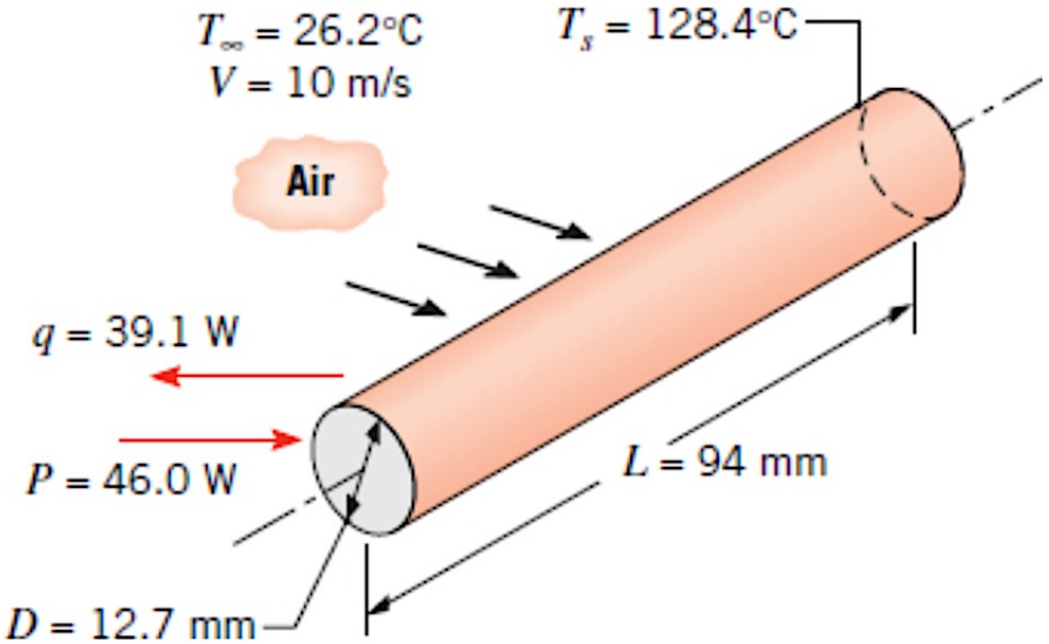

Assumptions:

1. Steady-state, incompressible flow conditions.

2. Uniform cylinder surface temperature.

Properties: Table A.4, air ($T_\infty = 26.2°C \approx 300$ K): $\nu = 15.89 \times 10^{-6}$ m^2/s, $k = 26.3 \times 10^{-3}$ W/m · K, $Pr = 0.707$. Table A.4, air ($T_f \approx 350$ K): $\nu = 20.92 \times 10^{-6}$ m^2/s, $k = 30 \times 10^{-3}$ W/m · K, $Pr = 0.700$. Table A.4, air ($T_s = 128.4°C = 401$ K): $Pr = 0.690$.

Analysis:

1. The convection heat transfer coefficient may be determined from the data by using Newton's law of cooling. That is,

$$h = \frac{q}{A(T_s - T_\infty)}$$

With $q = 0.85\,P$ and $A = \pi DL$, it follows that

$$h = \frac{0.85 \times 46\ \text{W}}{\pi \times 0.0127\ \text{m} \times 0.094\ \text{m}\ (128.4 - 26.2)°\text{C}} = 102\ \text{W/m}^2 \cdot \text{K} \quad \triangleleft$$

2. Working with the Zukauskas relation, Equation 7.53,

$$\text{Nu}_D = C\,\text{Re}_D^m\,\text{Pr}^n \left(\frac{\text{Pr}}{\text{Pr}_s}\right)^{1/4}$$

all properties, except Pr_s, are evaluated at T_∞. Accordingly,

$$\text{Re}_D = \frac{VD}{\nu} = \frac{10\ \text{m/s} \times 0.0127\ \text{m}}{15.89 \times 10^{-6}\ \text{m}^2/\text{s}} = 7992$$

Hence, from Table 7.4, $C = 0.26$ and $m = 0.6$. Also, since $Pr < 10$, $n = 0.37$. It follows that

$$\text{Nu}_D = 0.26(7992)^{0.6}\,(0.707)^{0.37}\left(\frac{0.707}{0.690}\right)^{0.25} = 50.5$$

$$h = \text{Nu}_D \frac{k}{D} = 50.5 \frac{0.0263\ \text{W/m} \cdot \text{K}}{0.0127\ \text{m}} = 105\ \text{W/m}^2 \cdot \text{K} \quad \triangleleft$$

Using the Churchill relation, Equation 7.54,

$$\mathrm{Nu}_D = 0.3 + \frac{0.62\,\mathrm{Re}_D^{1/2}\,\mathrm{Pr}^{1/3}}{[1+(0.4/\mathrm{Pr})^{2/3}]^{1/4}}\left[1+\left(\frac{\mathrm{Re}_D}{282{,}000}\right)^{5/8}\right]^{4/5}$$

With all properties evaluated at T_f, $Pr = 0.70$ and

$$\mathrm{Re}_D = \frac{VD}{\nu} = \frac{10\ \mathrm{m/s} \times 0.0127\ \mathrm{m}}{20.92 \times 10^{-6}\ \mathrm{m^2/s}} = 6071$$

Hence the Nusselt number and the convection coefficient are

$$\mathrm{Nu}_D = 0.3 + \frac{0.62(6071)^{1/2}(0.70)^{1/3}}{[1+(0.4/0.70)^{2/3}]^{1/4}}\left[1+\left(\frac{6071}{282{,}000}\right)^{5/8}\right]^{4/5} = 40.6$$

$$\bar{h} = \mathrm{Nu}_D\frac{k}{D} = 40.6\frac{0.030\ \mathrm{W/m \cdot K}}{0.0127\ \mathrm{m}} = 96.0\ \mathrm{W/m^2 \cdot K} \quad \triangleleft$$

Alternatively, from the Hilpert correlation, Equation 7.52,

$$\mathrm{Nu}_D = C\,\mathrm{Re}_D^m\,\mathrm{Pr}^{1/3}$$

With all properties evaluated at the film temperature, $Re_D = 6071$ and $Pr = 0.70$. Hence, from Table 7.2, $C = 0.193$ and $m = 0.618$. The Nusselt number and the convection coefficient are then

$$\mathrm{Nu}_D = 0.193(6071)^{0.618}(0.700)^{1/3} = 37.3$$

$$\bar{h} = \mathrm{Nu}_D\frac{k}{D} = 37.3\frac{0.030\ \mathrm{W/m \cdot K}}{0.0127\ \mathrm{m}} = 88.2\ \mathrm{W/m^2 \cdot K} \quad \triangleleft$$

Comments:

1. Calculations based on the three correlations are within the range of the measured value of the convection heat transfer coefficient, $\bar{h} = 102 \pm 20\ \mathrm{W/m^2 \cdot K}$.

2. Recognize the importance of using the proper temperature when evaluating fluid properties.

EXAMPLE 7.5

Hydrogen is often stored by *adsorbing* it into a metal hydride powder. The hydrogen can be desorbed as needed, by heating the metal hydride throughout its volume. Consider a hydrogen fuel cell-powered automobile cruising at a speed of $V = 25$ m/s. The car consumes $\dot{m}_{H_2} = 1.35 \times 10^{-4}$ kg/s of hydrogen, which is supplied from a cylindrical, stainless steel canister loaded with metal hydride powder. The canister is of inside diameter $D_i = 0.1$ m, length $L = 0.8$ m, and wall thickness $t = 0.5$ mm, and is subject to air in cross flow at $V = 25$ m/s, $T_\infty = 23°C$.

In order for desorption to occur, the metal hydride must be maintained at an operating temperature of at least 275 K. The desorption process is an endothermic reaction corresponding to a thermal generation rate expressed as

$$\dot{E}_g = -\dot{m}_{H_2} \times (29.5 \times 10^3 \text{ kJ/kg})$$

where $\dot{m}_{H_2}$ is the hydrogen desorption rate (kg/s). Determine how much additional heating, beyond that due to convection from the air, should be supplied to the canister to maintain the required operating temperature.

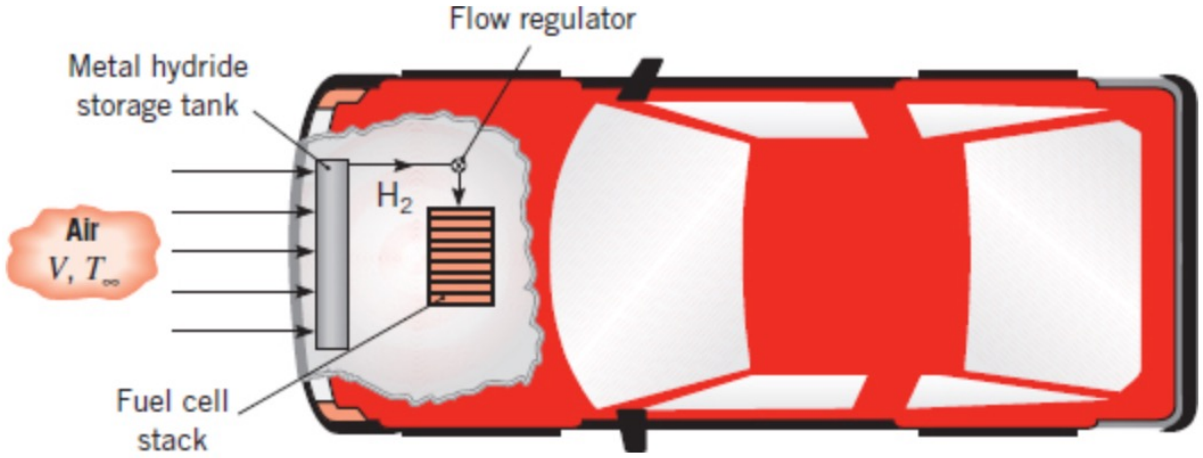

SOLUTION

Known: Size and shape of a hydrogen storage canister, hydrogen desorption rate, required hydroge pressure, velocity and temperature of air in cross flow.

Find: The rate of convective heat transfer to the canister and the additional heating needed to susta

Schematic:

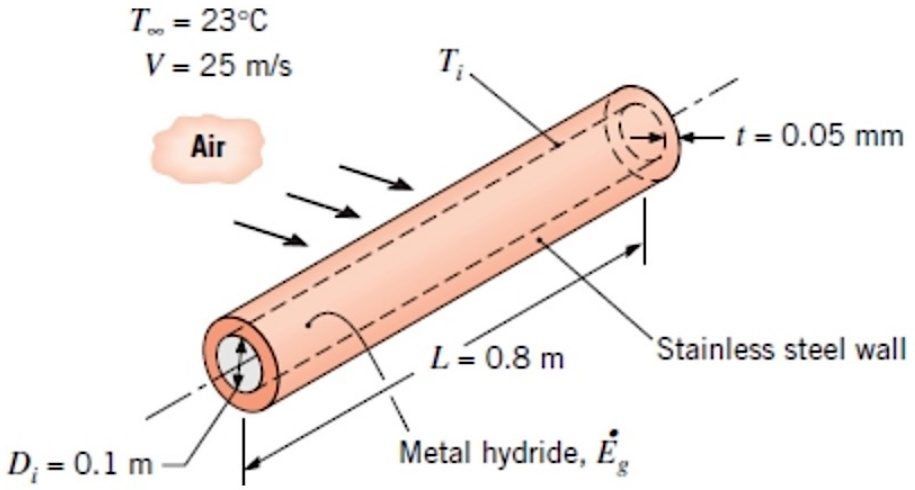

Assumptions:

1. Steady-state, incompressible flow conditions.

2. Uniform cylinder surface temperature.

3. Negligible heat gain through the ends of the cylinder.

4. Uniform metal hydride temperature.

5. Negligible contact resistance between the canister wall and the metal hydride.

Properties: Table A.4, air ($T_f \approx 285$ K): $\nu = 14.56 \times 10^{-6}$ m^2/s, $k = 25.2 \times 10^{-3}$ W/m · K, $Pr = 0.712$. Table A.1, AISI 316 stainless steel ($T_{ss} \approx 300$ K): $k_{ss} = 13.4$ W/m · K.

Analysis: The thermal energy generation rate associated with the desorption of hydrogen from the metal hydride at the required flow rate is

$$\dot{E}_g = -(1.35 \times 10^{-4}\ \text{kg/s}) \times (29.5 \times 10^{6}\ \text{J/kg}) = -3982\ \text{W}$$

To determine the convective heat transfer rate, we begin by calculating the Reynolds number:

$$\text{Re}_D = \frac{V(D_i + 2t)}{\nu} = \frac{23\ \text{m/s} \times (0.1\ \text{m} + 2 \times 0.005\ \text{m})}{14.56 \times 10^{-6}\ \text{m}^2/\text{s}} = 173{,}760$$

Use of Equation 7.54

$$\text{Nu}_D = 0.3 + \frac{0.62\ \text{Re}_D^{1/2}\ \text{Pr}^{1/3}}{[1 + (0.4/\text{Pr})^{2/3}]^{1/4}} \left[1 + \left(\frac{\text{Re}_D}{282{,}000}\right)^{5/8}\right]^{4/5}$$

yields

$$\text{Nu}_D = 0.3 + \frac{0.62(173{,}760)^{1/2}\,(0.712)^{1/3}}{[1 + (0.4/0.712)^{2/3}]^{1/4}} \left[1 + \left(\frac{173{,}760}{282{,}000}\right)^{5/8}\right]^{4/5} = 315.8$$

Therefore, the average convection heat transfer coefficient is

$$\bar{h} = \text{Nu}_D \frac{k}{(D_i + 2t)} = 315.8 \times \frac{25.3 \times 10^{-3}\ \text{W/m} \cdot \text{K}}{(0.1\ \text{m} + 2 \times 0.005\ \text{m})} = 72.6\ \text{W/m}^2 \cdot \text{K}$$

Simplifying Equation 3.34, we find

$$q_{\text{conv}} = \frac{T_\infty - T_i}{\dfrac{1}{\pi L (D_i + 2t)\bar{h}} + \dfrac{\ln[(D_i + 2t)/D_i]}{2\pi k_{ss} L}}$$

or, substituting values,

$$q_{\text{conv}} = \frac{296\ \text{K} - 275.2\ \text{K}}{\dfrac{1}{\pi(0.8\ \text{m})(0.1\ \text{m} + 2 \times 0.005\ \text{m})(72.6\ \text{W/m}^2 \cdot \text{K})} + \dfrac{\ln[(0.1\ \text{m} + 2 \times 0.005\ \text{m})/0.1\ \text{m}]}{2\pi(13.4\ \text{W/m} \cdot \text{K})(0.8\ \text{m})}}$$
$$= 406\ \text{W}$$

The additional thermal energy, q_{add}, that must be supplied to the canister to maintain the steady-state operating temperature may be found from an energy balance, $q_{\text{add}} + q_{\text{conv}} + \dot{E}_g = 0$. Therefore,

$$q_{\text{add}} = -q_{\text{conv}} - \dot{E}_g = -406\ \text{W} + 3982\ \text{W} = 3576\ \text{W} \quad \triangleleft$$

Comments:

1. Additional heating will occur due to radiation, conduction from the canister mounting hardware and fuel lines, and possibly condensation of water vapor on the cool canister.

2. The thermal resistances associated with conduction in the canister wall and convection are 0.0014 K/W and 0.053 K/W, respectively. The convection resistance dominates and can be reduced by adding fins to the exterior of the canister.

3. The amount of additional heating that is required will increase if the automobile is operated at a higher speed, since the hydrogen consumption scales as V^3, while the convective heat transfer coefficient increases as $V^{0.7}$ to $V^{0.8}$. Additional heating is also needed when the automobile is operated in a cooler climate.

The Sphere

Boundary layer effects associated with flow over a sphere are much like those for the circular cylinder, with transition and separation playing prominent roles.

$$C_D = \frac{24}{\mathrm{Re}_D} \quad \mathrm{Re}_D \lesssim 0.5$$

$$\mathrm{Nu}_D = 2 + (0.4\,\mathrm{Re}_D^{1/2} + 0.06\,\mathrm{Re}_D^{2/3})\mathrm{Pr}^{0.4}\left(\frac{\mu}{\mu_s}\right)^{1/4}$$

$$\begin{bmatrix} 0.71 \lesssim \mathrm{Pr} \lesssim 380 \\ 3.5 \lesssim \mathrm{Re}_D \lesssim 7.6 \times 10^4 \\ 1.0 \lesssim (\mu/\mu_s) \lesssim 3.2 \end{bmatrix}$$

$$\mathrm{Nu}_D = 2 + 0.6\,\mathrm{Re}_D^{1/2}\,\mathrm{Pr}^{1/3}$$

All properties except μs are evaluated at T∞,

EXAMPLE 7.6

Electrical circuitry is written onto a photovoltaic panel by depositing a stream of small ($D = 55\ \mu m$) droplets of electrically conducting ink from a thermal inkjet printer. The drops are at an initial temperature of $T_i = 200°C$, and it is desirable for them to strike the panel at a temperature of $T_{final} = 50°C$. The quiescent air and surroundings are at $T_\infty = T_{sur} = 25°C$, and the drops are ejected from the print head at their terminal velocity. Determine the required standoff distance L between the printer and the photovoltaic panel. The properties of the electrically conducting ink drop are $\rho_d = 2400\ kg/m^3$, $c_d = 800\ J/kg \cdot K$, and $k_d = 5.0\ W/m \cdot K$.

SOLUTION

Known: Droplet size and properties, initial and desired final droplet temperature. Droplet injected at its terminal velocity.

Find: Required standoff distance between the printer and the photovoltaic panel.

Schematic:

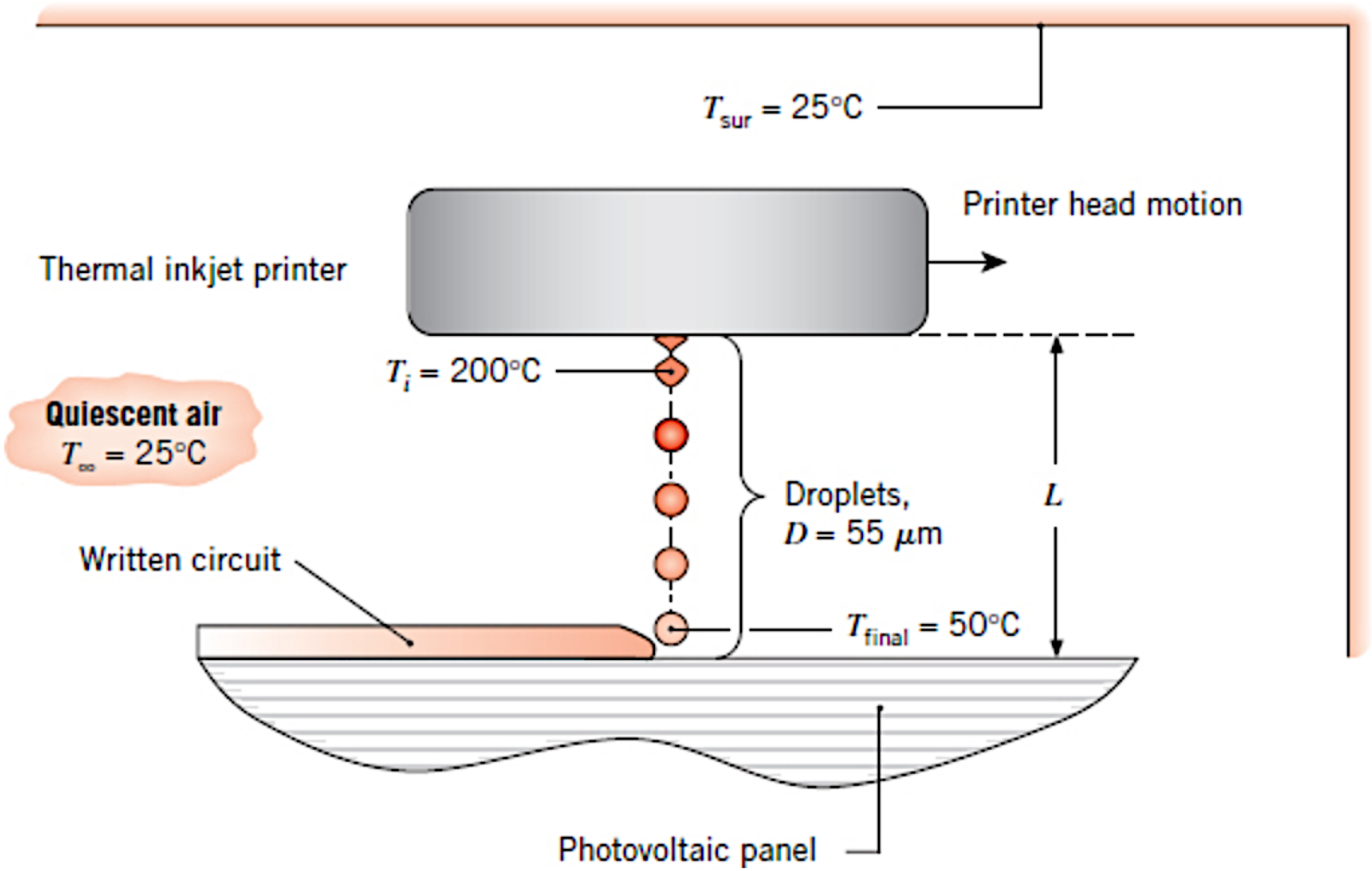
T_{sur} = 25°C
Printer head motion
Thermal inkjet printer
T_i = 200°C
Quiescent air
T_∞ = 25°C
Droplets,
D = 55 μm
L
Written circuit
T_{final} = 50°C
Photovoltaic panel

Assumptions:

1. Constant air properties evaluated at 25°C.

2. Negligible radiation effects.

3. Negligible temperature variation within the droplets (lumped capacitance approximation).

Properties: Table A.4, air ($T_f = 75°C$): $\rho = 1.002$ kg/m^3, $\nu = 20.72 \times 10^{-6}$ m^2/s. Table A.4, air ($T_\infty = 25°C$): $\nu = 15.71 \times 10^{-6}$ m^2/s, $k = 0.0261$ W/m · K, $Pr = 0.708$.

Analysis: Since the droplets travel at their terminal velocities, the net force on each drop must be zero. Hence the weight of the drop is offset by the buoyancy force associated with the displaced air and the drag force:

$$\rho_d g\left(\pi\frac{D^3}{6}\right) = \rho g\left(\pi\frac{D^3}{6}\right) + C_D\left(\frac{\pi D^2}{4}\right)\left(\rho\frac{V^2}{2}\right) \tag{1}$$

where Equation 7.50 has been used to express the drag force F_D. Since the droplets are small, we anticipate that the Reynolds number will also be small. If this is the case, Stokes' law, Equation 7.55 may be used to express the drag coefficient as

$$C_D = \frac{24}{\mathrm{Re}_D} = \frac{24\nu}{VD} \tag{2}$$

Substituting Equation (2) into Equation (1) and solving for the velocity,

$$V = \frac{gD^2}{18\nu\rho}(\rho_d - \rho) = \frac{9.8\ \mathrm{m/s^2} \times (55 \times 10^{-6}\ \mathrm{m})^2}{18 \times 20.72 \times 10^{-6}\ \mathrm{m^2/s} \times 1.002\ \mathrm{kg/m^3}} \times (2400 - 1.002)\mathrm{kg/m^3}$$

$$= 0.190\ \mathrm{m/s} = 190\ \mathrm{mm/s}$$

Therefore, the Reynolds number is $Re_D = VD/\nu = 0.190\ \text{m/s} \times 55 \times 10^{-6}\ \text{m}/20.72 \times 10^{-6}\ \text{m}^2/\text{s} = 0.506$, and use of Stokes' law is appropriate. The Nusselt number and convection coefficient can be calculated from the Ranz and Marshall correlation, Equation 7.57, using properties evaluated at the free stream temperature (see Table 7.7):

$$\text{Nu}_D = 2 + 0.6\,\text{Re}_D^{1/2}\,\text{Pr}^{1/3} = 2 + 0.6 \times \left(\frac{0.190\ \text{m/s} \times 55 \times 10^{-6}\ \text{m}}{15.71 \times 10^{-6}\ \text{m}^2/\text{s}}\right)^{1/2} \times 0.708^{1/3} = 2.44$$

$$\bar{h} = \frac{\text{Nu}_D\, k}{D} = \frac{2.44 \times 0.0261\ \text{W/m} \cdot \text{K}}{55 \times 10^{-6}\ \text{m}} = 1160\ \text{W/m}^2 \cdot \text{K}$$

Applying the lumped capacitance method, Equation 5.5, the required *time-of-flight* is then

$$\begin{aligned} t &= \frac{\rho_d V c_d}{\bar{h} A_s} \ln\left(\frac{\theta_i}{\theta_{\text{final}}}\right) = \frac{\rho_d c_d D}{6\bar{h}} \ln\left(\frac{T_i - T_\infty}{T_{\text{final}} - T_\infty}\right) \\ &= \frac{2400\ \text{kg/m}^3 \times 800\ \text{J/kg} \cdot \text{K} \times 55 \times 10^{-6}\ \text{m}}{6 \times 1160\ \text{W/m}^2 \cdot \text{K}} \ln\left(\frac{(200 - 25)^\circ\text{C}}{(50 - 25)^\circ\text{C}}\right) \\ &= 0.030\ \text{s} \end{aligned}$$

and the standoff distance is

$$L = Vt = 0.190\ \text{m/s} \times 0.030\ \text{s} = 0.0056\ \text{m} = 5.6\ \text{mm} \qquad \triangleleft$$

Comments:

1. The validity of the lumped capacitance method may be determined by calculating the Biot number. Applying Equation 5.10 in the conservative fashion with $L_c = D/2$,

$$\text{Bi} = \frac{\bar{h}(D/2)}{k_p} = \left(\frac{1160\ \text{W/m}^2 \cdot \text{K} \times 55 \times 10^{-6}\ \text{m}}{2}\right) / 5.0\ \text{W/m} \cdot \text{K} = 0.006 < 0.1$$

and the criterion is satisfied.

2. Use of Equation 7.55, Stokes' law, to describe the Reynolds number dependence of the drag coefficient is valid since $Re_D \lesssim 0.5$. For larger particles, Figure 7.9 would need to be consulted to determine the relationship between C_D and Re_D.

3. If the particles were not injected at their terminal velocity, they would either accelerate or decelerate during flight, complicating the analysis.

4. Assuming blackbody behavior and using the maximum (initial) temperature of the particle, $T_s = 473$ K, the maximum radiation heat transfer coefficient is

$$h_r = \sigma(T_s + T_{sur})(T_s^2 + T_{sur}^2) = 5.67 \times 10^{-8}\ \text{W/m}^2 \cdot \text{K}^4 \times (473\ \text{K} + 298\ \text{K}) \times [(473\ \text{K})^2 + (298\ \text{K})^2] = 13.7\ \text{W/m}^2 \cdot \text{K}.$$

Since $h_r \ll h$, radiation heat transfer is negligible.

Flow Across Banks of Tubes

Heat transfer to or from a bank (or bundle) of tubes in cross flow is relevant to numerous industrial applications, such as **steam generation in a boiler** or **air cooling in the coil of an air conditioner**.

The geometric arrangement is shown schematically in Figure 7.11. Typically, one fluid moves over the tubes, while a second fluid at a different temperature passes through the tubes.

In this section we are specifically interested in the convection heat transfer associated with cross flow over the tubes.

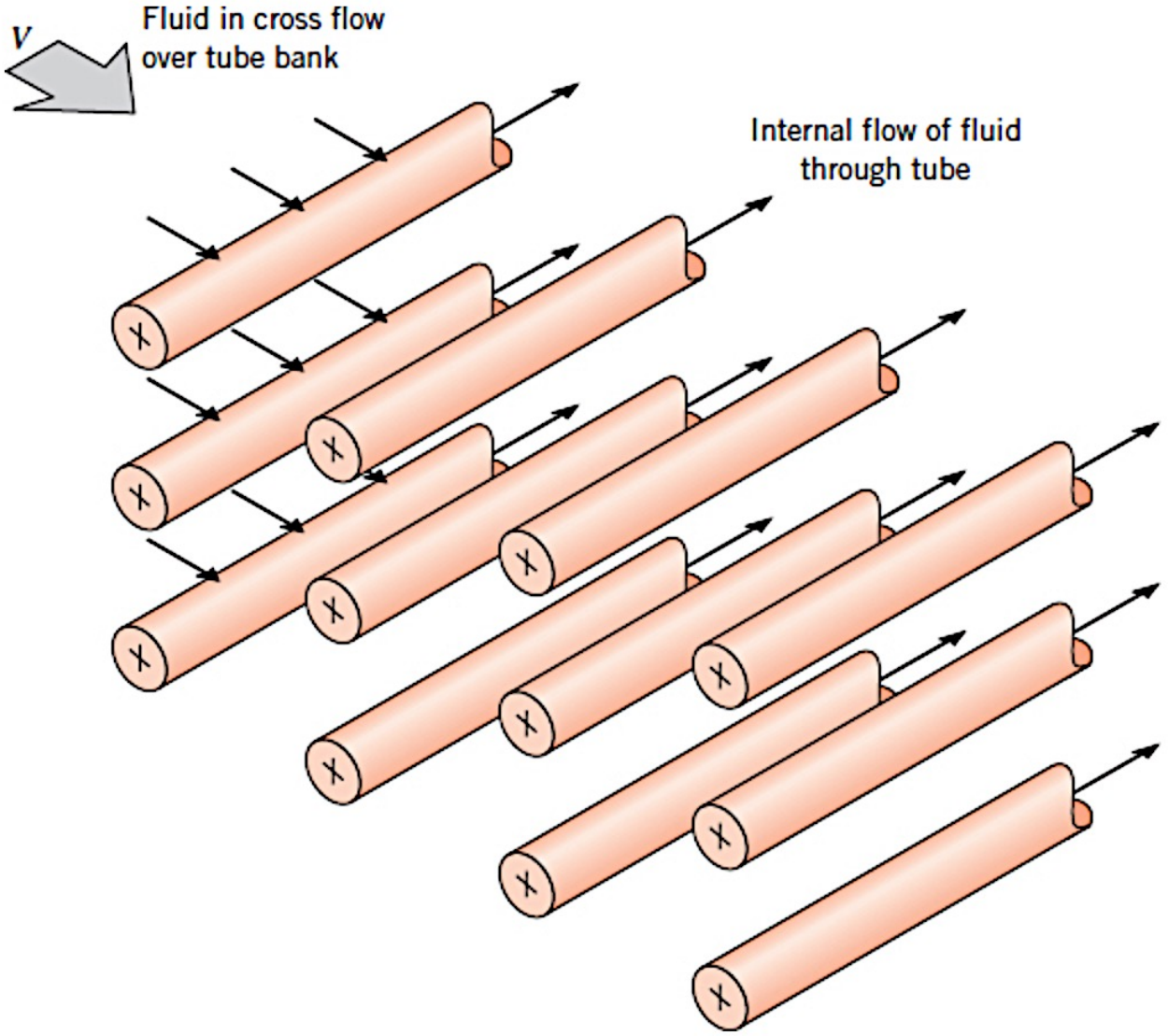

FIGURE 7.11 Schematic of a tube bank in cross flow.

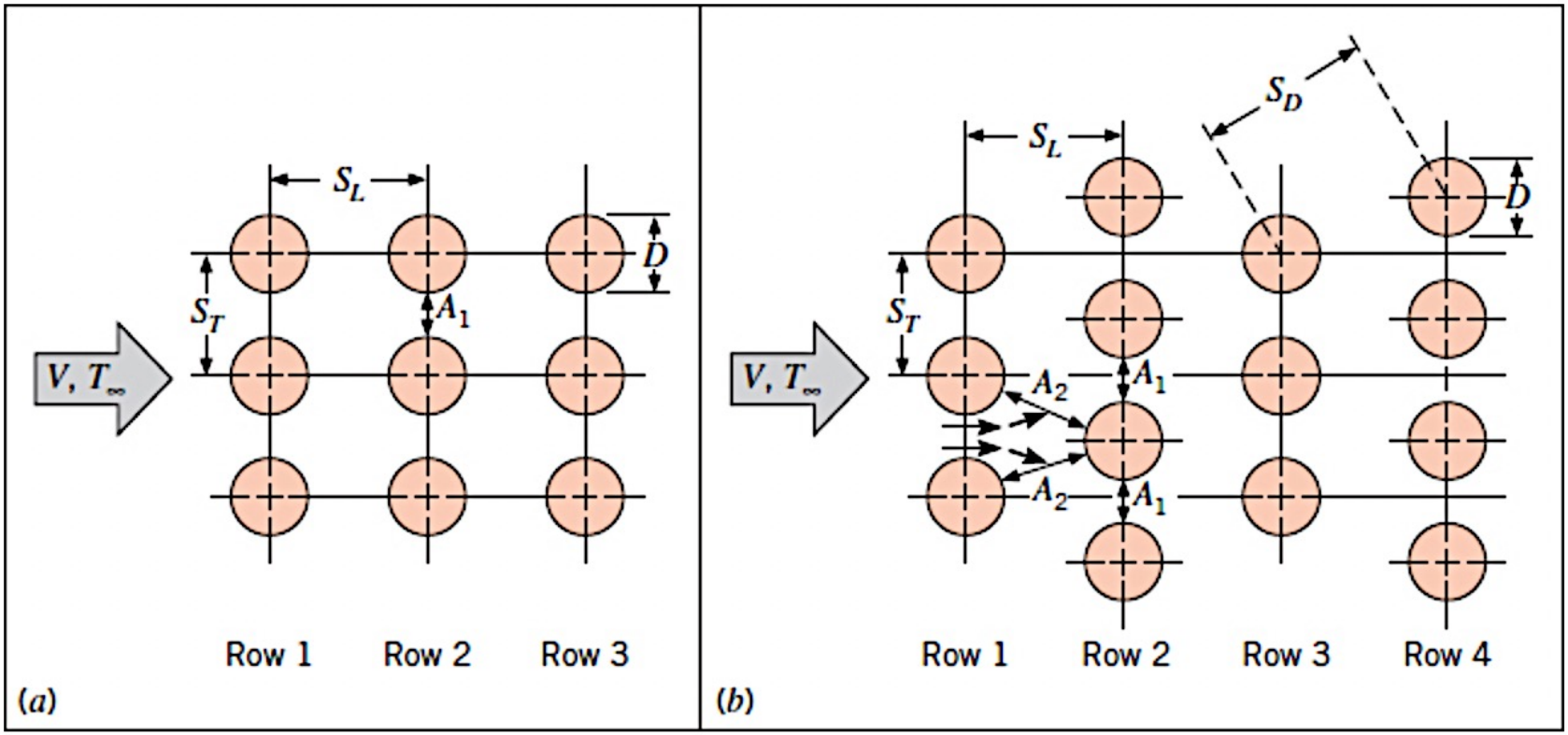

FIGURE 7.12 Tube arrangements in a bank. (*a*) Aligned. (*b*) Staggered.

The tube rows of a bank can be either aligned or staggered in the direction of the fluid velocity V (Figure 7.12).

The configuration is characterized by the tube diameter D and by the transverse pitch ST and longitudinal pitch SL measured between tube centers.

Flow conditions within the bank are dominated by boundary layer separation effects and by wake interactions, which in turn influence convection heat transfer.

Flow around the tubes in the first row of a tube bank is similar to that for a single (isolated) cylinder in cross flow.

Correspondingly, the **heat transfer coefficient for a tube in the first row** is approximately **equal to that for a single tube in cross flow.**

For downstream rows, flow conditions depend strongly on the tube bank arrangement (Figure 7.13). Aligned tubes beyond the first row reside in the wakes of upstream tubes, and for moderate values of S_L convection coefficients associated with downstream rows are enhanced by mixing, or turbulation, of the flow.

Typically, **the convection coefficient of a row increases with increasing row number until approximately the fifth row**, after which there is little change in flow conditions and hence in the convection coefficient.

For large SL, the influence of upstream rows decreases, and heat transfer in the downstream rows is not enhanced.

For this reason, operation of aligned tube banks with $ST/SL < 0.7$ is undesirable.

For the staggered tube array, the path of the main flow is more tortuous, and mixing of the cross-flowing fluid is increased relative to the aligned tube arrangement.

In general, heat transfer enhancement is favored by the more tortuous flow of a staggered arrangement, particularly for small Reynolds numbers ($ReD \lesssim 100$).

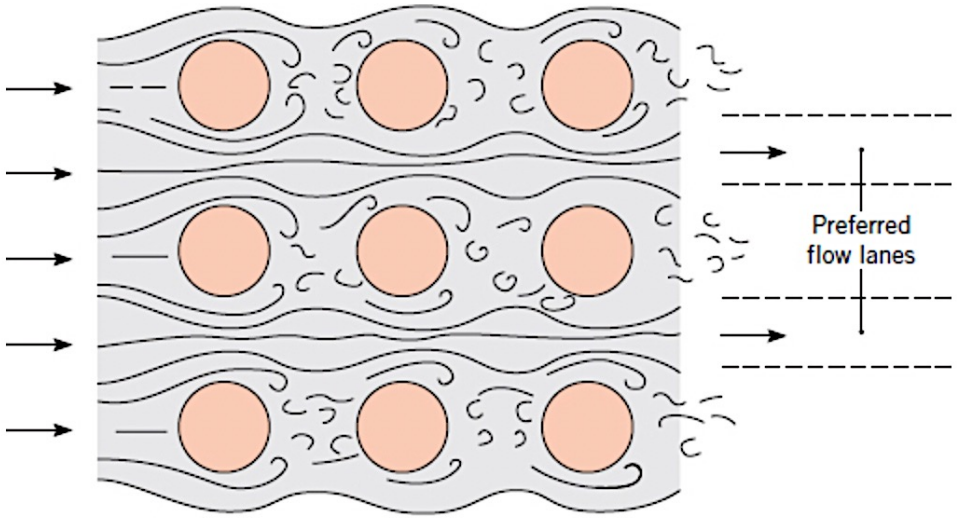

(*a*)

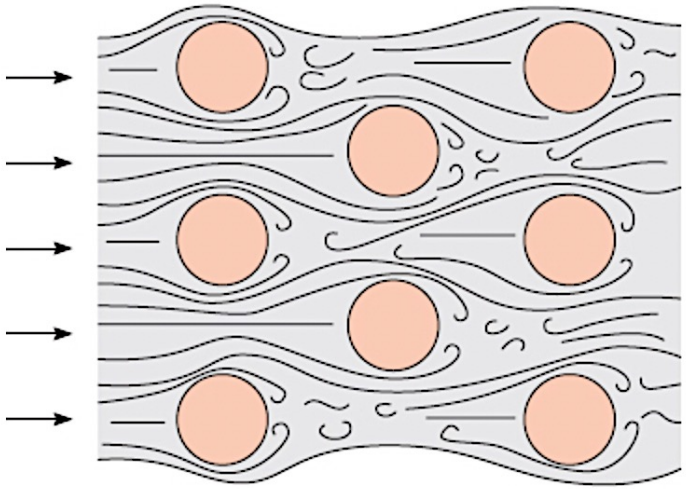

(*b*)

FIGURE 7.13 Flow conditions for (*a*) aligned and (*b*) staggered tubes.

Typically, we wish to know the average heat transfer coefficient for the entire tube bank. A correlation has been proposed of the form

$$\mathrm{Nu}_D = C_1 \, \mathrm{Re}_{D,\max}^{m} \, \mathrm{Pr}^{0.36} \left(\frac{\mathrm{Pr}}{\mathrm{Pr}_s} \right)^{1/4}$$

$$\begin{bmatrix} N_L \geq 20 \\ 0.7 \lesssim \mathrm{Pr} \lesssim 500 \\ 10 \lesssim \mathrm{Re}_{D,\max} \lesssim 2 \times 10^6 \end{bmatrix}$$

where N_L is the number of tube rows, all properties except Pr_s are evaluated at the **arithmetic mean** of **the fluid inlet ($T_i = T_\infty$) and outlet (To) temperatures**, and the constants C1 and m are listed in Table 7.5

TABLE 7.5 Constants of Equation 7.58 for the tube bank in cross flow [17]

Configuration	$Re_{D,max}$	C_1	m
Aligned	$10 - 10^2$	0.80	0.40
Staggered	$10 - 10^2$	0.90	0.40
Aligned Staggered	$10^2 - 10^3$ $10^2 - 10^3$	Approximate as a single (isolated) cylinder	
Aligned ($S_T/S_L > 0.7$)[a]	$10^3 - 2 \times 10^5$	0.27	0.63
Staggered ($S_T/S_L < 2$)	$10^3 - 2 \times 10^5$	$0.35(S_T/S_L)^{1/5}$	0.60
Staggered ($S_T/S_L > 2$)	$10^3 - 2 \times 10^5$	0.40	0.60
Aligned	$2 \times 10^5 - 2 \times 10^6$	0.021	0.84
Staggered	$2 \times 10^5 - 2 \times 10^6$	0.022	0.84

For ST/SL < 0.7, heat transfer is inefficient and aligned tubes should not be used.

If there are 20 or fewer rows of tubes, $N_L \lesssim 20$, the average heat transfer coefficient is typically reduced relative to banks with more tube rows, and a correction factor may be applied such that

$$\overline{Nu}_D\Big|_{(N_L < 20)} = C_2 \overline{Nu}_D|_{(N_L \geq 20)}$$

where C_2 is given in Table 7.6.

TABLE 7.6 Correction factor C_2 of Equation 7.59 for $N_L < 20$ ($Re_{D,max} \approx 10^3$) [17]

N_L	1	2	3	4	5	7	10	13	16
Aligned	0.70	0.80	0.86	0.90	0.92	0.95	0.97	0.98	0.99
Staggered	0.64	0.76	0.84	0.89	0.92	0.95	0.97	0.98	0.99

The Reynolds number $Re_{D,\,max}$ for the foregoing correlation is based on the maximum fluid velocity occurring within the tube bank, $Re_{D,\,max} \equiv \rho V_{max} D/\mu$. **For the aligned arrangement, V_{max} occurs at the transverse plane A_1** of Figure 7.12a, and from the mass conservation requirement for a constant density fluid

$$V_{max} = \frac{S_T}{S_T - D} V \qquad \text{Equation 7.60.}$$

For the staggered configuration**, the maximum velocity may occur** at either the transverse plane **A_1 or the diagonal plane A_2** of Figure 7.12b.

It will occur at **A_2 if** the rows are spaced such that

$$2(S_D - D) < (S_T - D)$$

V_{max} occurs at A_2 if $$S_D = [S_L^2 + \left(\frac{S_T}{2}\right)^2]^{1/2} < \frac{S_T + D}{2}$$

$$V_{max} = \frac{S_T}{2(S_D - D)}V$$

If the maximum velocity occurs at **A_1:**

$$V_{max} = \frac{S_T}{S_T - D}V$$

Since the fluid may experience a large change in temperature as it moves through the tube bank, the **heat transfer rate could be significantly overpredicted by using $\Delta T = Ts - T\infty$** as the temperature difference in Newton's law of cooling. As the fluid moves through the bank, its temperature approaches Ts and $|\Delta T|$ decreases. The appropriate form of ΔT is shown to be a **log-mean temperature difference,**

$$\Delta T_{\text{lm}} = \frac{(T_s - T_i) - (T_s - T_o)}{\ln\left(\frac{T_s - T_i}{T_s - T_o}\right)}$$

where Ti and To are temperatures of the fluid as it enters and leaves the bank, respectively. **The outlet temperature, which is needed to determine ΔT_{lm}, may be estimated from**

$$\frac{T_s - T_o}{T_s - T_i} = \exp\left(-\frac{\pi D N \bar{h}}{\rho V N_T S_T c_p}\right)$$

where N is the total number of tubes in the bank and N_T is **the number of tubes in each row**. Once ΔT_{lm} is known, **the heat transfer rate per unit length of the tubes** may be computed from

$$q' = N(h\pi D\Delta T_{lm})$$

We close by recognizing that there is generally as much interest in **the pressure drop associated with flow across a tube bank** as in the overall heat transfer rate.

The power required to move the fluid across the bank is often a major operating expense and is directly proportional to the pressure drop, which may be expressed

$$\Delta p = N_L \chi \left(\frac{\rho V_{\max}^2}{2} \right) f$$

The friction factor f and the correction factor χ are plotted in Figures 7.14 and 7.15. Figure 7.14 **pertains to a square, in-line tube arrangement for which the dimensionless longitudinal and transverse pitches**, $P_L \equiv S_L/D$ and $P_T \equiv S_T/D$, respectively, are equal.

The correction factor χ, plotted in the inset, is used to apply the results to other in-line arrangements.

Similarly, Figure 7.15 applies to a staggered arrangement of tubes in the form of an equilateral triangle (ST = SD), and the correction factor enables extension of the results to other staggered arrangements.

Note that the Reynolds number appearing in Figures 7.14 and 7.15 is based on the maximum fluid velocity Vmax.

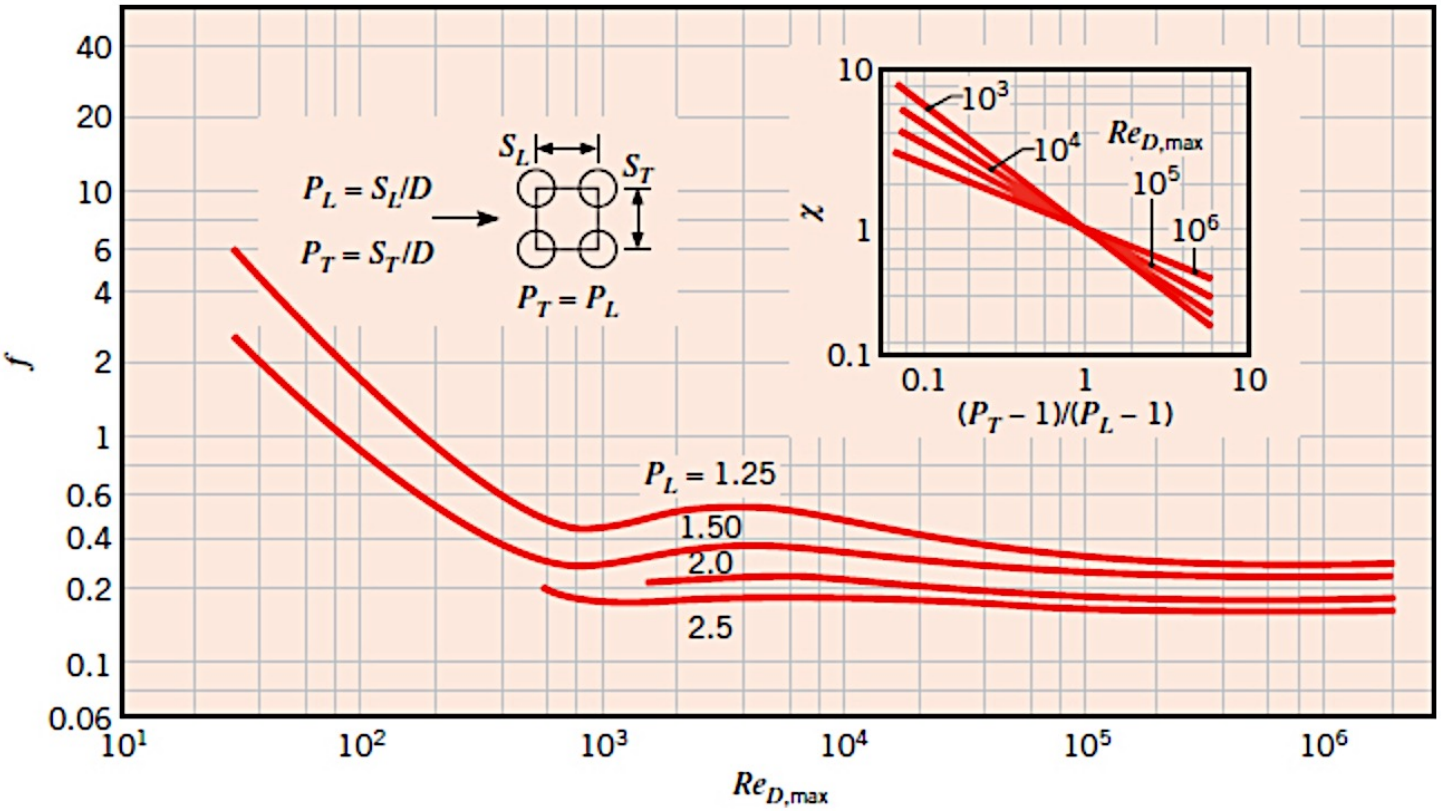

FIGURE 7.14 Friction factor f and correction factor χ for Equation 7.65. In-line tube bundle arrangement [17]. (Used with permission.)

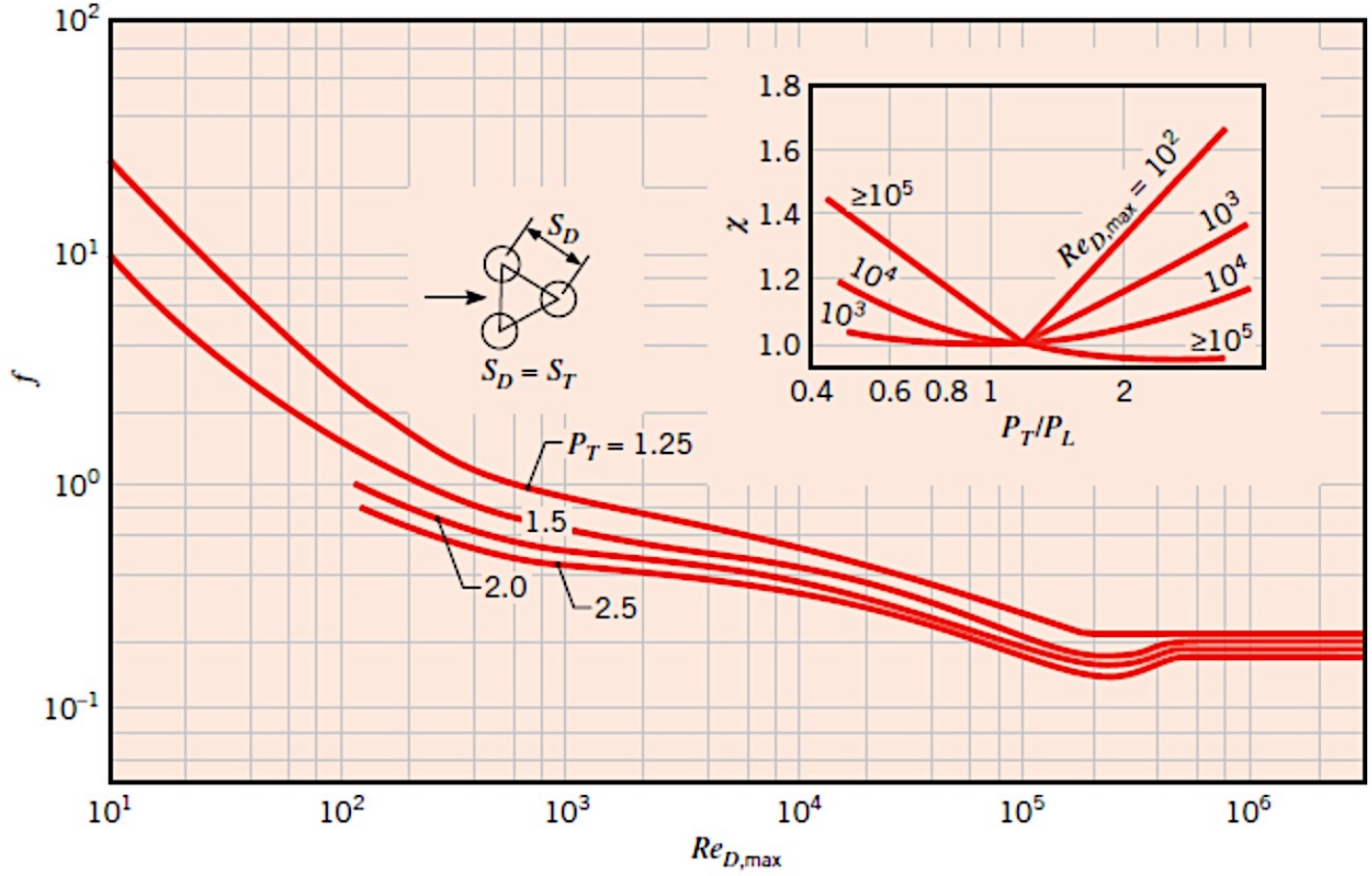

FIGURE 7.15 Friction factor f and correction factor χ for Equation 7.65. Staggered tube bundle arrangement [17]. (Used with permission.)

Example 7.7

Pressurized water is often available at elevated temperatures and may be used for space heating or industrial process applications. In such cases it is customary to use a tube bundle in which the water is passed through the tubes, while air is passed in cross flow over the tubes. Consider a staggered arrangement for which the tube outside diameter is 16.4 mm and the longitudinal and transverse pitches are $S_L = 34.3$ mm and $S_T = 31.3$ mm. There are seven rows of tubes in the airflow direction and eight tubes per row. Under typical operating conditions the cylinder surface temperature is at 70°C, while the air upstream temperature and velocity are 15°C and 6 m/s, respectively. Determine the air-side convection coefficient and the rate of heat transfer for the tube bundle. What is the air-side pressure drop?

Solution

Known: Geometry and operating conditions of a tube bank.

Find:

1. Air-side convection coefficient and heat rate.

2. Pressure drop.

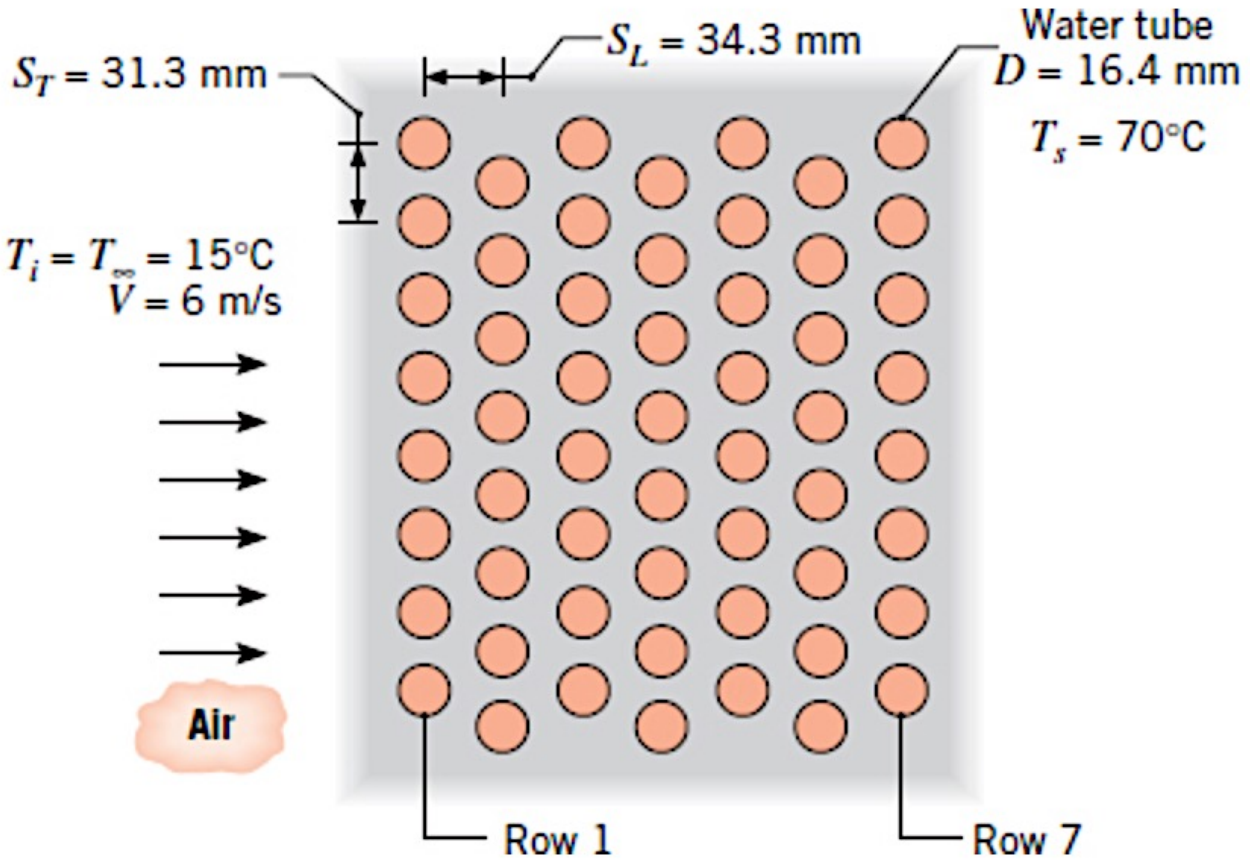
S_T = 31.3 mm
S_L = 34.3 mm
Water tube
D = 16.4 mm
T_s = 70°C
$T_i = T_\infty$ = 15°C
V = 6 m/s
Air
Row 1
Row 7

Assumptions:

1. Steady-state, incompressible flow conditions.

2. Negligible radiation effects.

3. Negligible effect of change in air temperature across tube bank on air properties.

Properties: Table A.4, air ($T_\infty = 15°C$): $\rho = 1.217$ kg/m^3, $c_p = 100^7$ J/kg · K, $\nu = 14.82 \times 10^{-6}$ m^2/s, $k = 0.0253$ W/m · K, $Pr = 0.710$. Table A.4, air ($T_s = 70°C$): $Pr = 0.701$. Table A.4, air ($T_f = 43°C$): $\nu = 17.4 \times 10^{-6}$ m^2/s, $k = 0.0274$ W/m · K, $Pr = 0.705$.

Analysis:

1. From Equations 7.58 and 7.59, the air-side Nusselt number is

$$\overline{\mathrm{Nu}}_D = C_2\, C_1\, \mathrm{Re}_{D,\max}^{m}\, \mathrm{Pr}^{0.36} \left(\frac{\mathrm{Pr}}{\mathrm{Pr}_s}\right)^{1/4}$$

Since $S_D = [S_L^2 + (S_T/2)^2]^{1/2} = 37.7$ mm is greater than $(S_T + D)/2$, the maximum velocity occurs on the transverse plane, A_1, of Figure 7.12. Hence from Equation 7.60

$$V_{\max} = \frac{S_T}{S_T - D} V = \frac{31.3 \text{ mm}}{(31.3 - 16.4) \text{ mm}} 6 \text{ m/s} = 12.6 \text{ m/s}$$

With

$$\mathrm{Re}_{D,\max} = \frac{V_{\max} D}{\nu} = \frac{12.6 \text{ m/s} \times 0.0164 \text{ m}}{14.82 \times 10^{-6} \text{ m}^2/\text{s}} = 13{,}943$$

and

$$\frac{S_T}{S_L} = \frac{31.3 \text{ mm}}{34.3 \text{ mm}} = 0.91 < 2$$

it follows from Tables 7.5 and 7.6 that

$$C_1 = 0.35\left(\frac{S_T}{S_L}\right)^{1/5} = 0.34, \quad m = 0.60, \quad \text{and} \quad C_2 = 0.95$$

Hence

$$\text{Nu}_D = 0.95 \times 0.34(13{,}943)^{0.60}\,(0.71)^{0.36}\left(\frac{0.710}{0.701}\right)^{0.25} = 87.9$$

and

$$h = \text{Nu}_D \frac{k}{D} = 87.9 \times \frac{0.0253\ \text{W/m} \cdot \text{K}}{0.0164\ \text{m}} = 135.6\ \text{W/m}^2 \cdot \text{K} \quad \triangleleft$$

From Equation 7.63

$$\begin{aligned} T_s - T_o &= (T_s - T_i)\exp\left(-\frac{\pi D N h}{\rho V N_T S_T c_p}\right) \\ T_s - T_o &= (55°\text{C})\exp\left(-\frac{\pi(0.0164\ \text{m})56\ (135.6\ \text{W/m}^2 \cdot \text{K})}{1.217\ \text{kg/m}^3\ (6\ \text{m/s})\ 8\ (0.0313\ \text{m})\ 1007\ \text{J/kg} \cdot \text{K}}\right) \\ T_s - T_o &= 44.5°\text{C} \end{aligned}$$

Hence from Equations 7.62 and 7.64

$$\Delta T_{\text{lm}} = \frac{(T_s - T_i) - (T_s - T_o)}{\ln\left(\frac{T_s - T_i}{T_s - T_o}\right)} = \frac{(55 - 44.5)°\text{C}}{\ln\left(\frac{55}{44.5}\right)} = 49.6°\text{C}$$

and

$$\begin{aligned} q' &= N(h\pi D\Delta T_{\text{lm}}) = 56\pi \times 135.6\ \text{W/m}^2 \cdot \text{K} \times 0.0164\ \text{m} \times 49.6°\text{C} \\ q' &= 19.4\ \text{kW/m} \end{aligned} \quad \triangleleft$$

2. The pressure drop may be obtained from Equation 7.65.

$$\Delta p = N_L \chi \left(\frac{\rho V_{\max}^2}{2} \right) f$$

With $Re_{D,\,\max} = 13{,}943$, $P_T = (S_T/D) = 1.91$, $P_L = (S_L/D) = 2.09$, and $(P_T/P_L) = 0.91$, it follows from Figure 7.15 that $\chi \approx 1.04$ and $f \approx 0.35$. Hence with $N_L = 7$

$$\Delta p = 7 \times 1.04 \left[\frac{1.217\ \text{kg/m}^3\ (12.6\ \text{m/s})^2}{2} \right] 0.35$$

$$\Delta p = 246\ \text{N/m}^2 = 2.46 \times 10^{-3}\ \text{bars} \qquad \triangleleft$$

Comments:

1. Had $\Delta T_i \equiv T_s - T_i$ been used in lieu of ΔT_{lm} in Equation 7.64, the heat rate would have been overpredicted by 11%.

2. Since the air temperature is predicted to increase by only 10.5°C, evaluation of the air properties at $T_i = 15$°C is a reasonable approximation. However, if improved accuracy is desired, the calculations could be repeated with the properties reevaluated at $(T_i + T_o)/2 = 20.25$°C. An exception pertains to the density ρ in the exponential term of Equation 7.63. As it appears in the denominator of this term, ρ is matched with the inlet velocity to provide a product (ρV) that is linked to the mass flow rate of air entering the tube bank. Hence, in this term, ρ should be evaluated at T_i.

3. The air outlet temperature and heat rate may be increased by increasing the number of tube rows, and for a fixed number of rows, they may be varied by adjusting the air velocity. For $5 \le N_L \le 25$ and $V = 6$ m/s, parametric calculations based on Equations 7.58, 7.59, and 7.62 through 7.64 yield the following results:

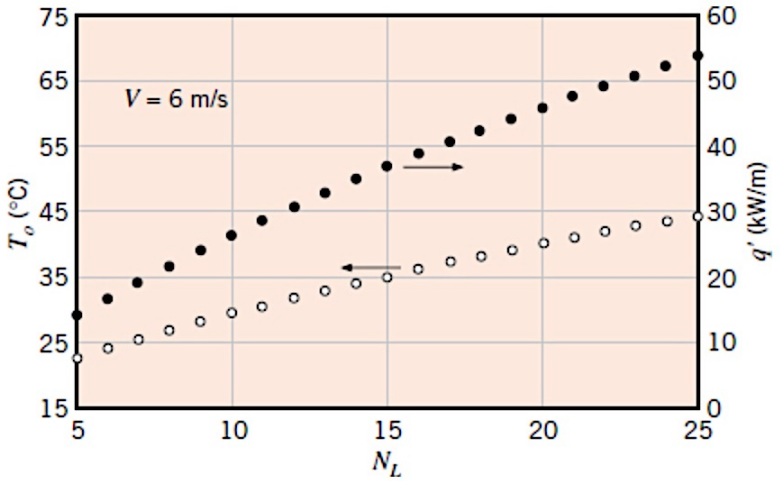

The air outlet temperature would asymptotically approach the surface temperature with increasing N_L, at which point the heat rate approaches a constant value and there is no advantage to adding more tube rows. Note that Δp increases linearly with increasing N_L. For $N_L = 25$ and $1 \le V \le 20$ m/s, we obtain

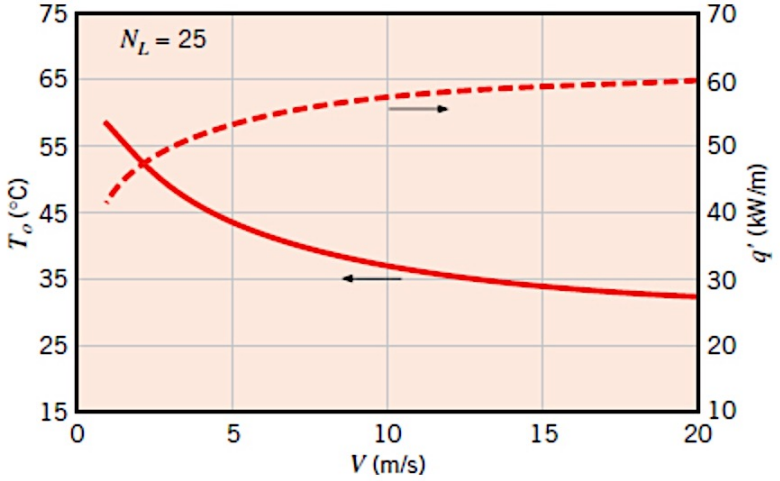

Although the heat rate increases with increasing V, the air outlet temperature decreases, approaching T_i as $V \to \infty$.

Chapter 8
Internal Flow

Velocity boundary layer:

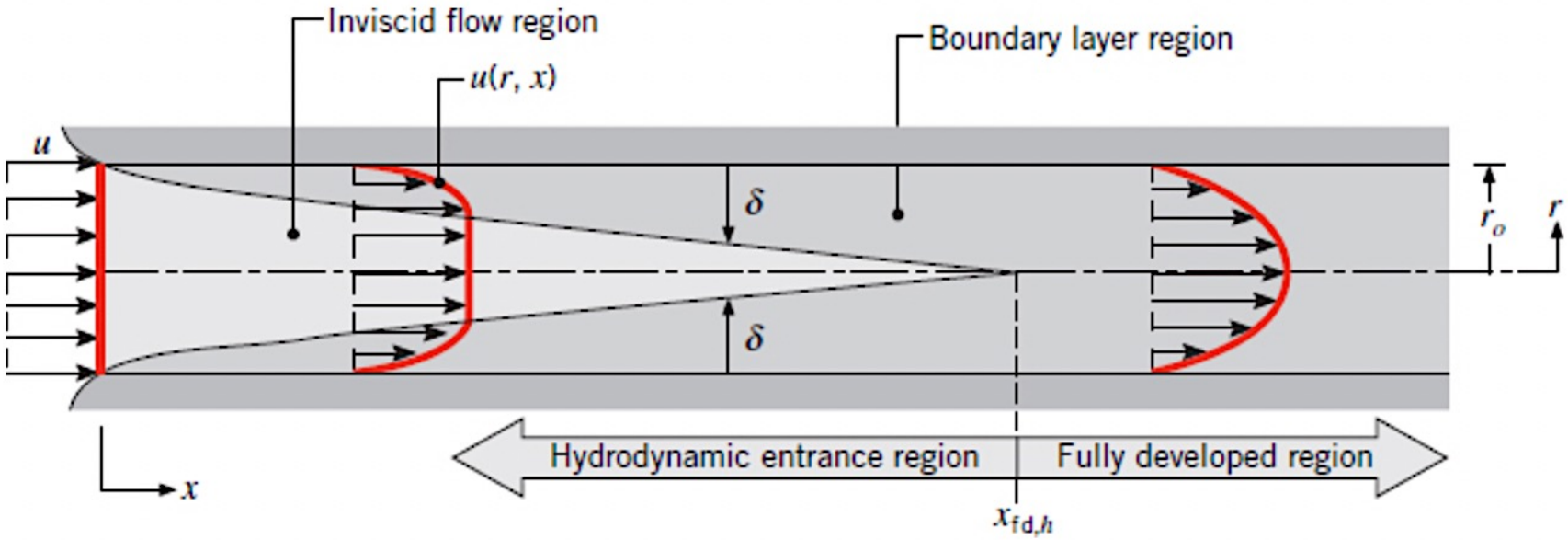

FIGURE 8.1 Laminar, hydrodynamic boundary layer development in a circular tube.

This development occurs at the expense of a shrinking inviscid flow region and concludes with boundary layer merger at the centerline. Following this merger, viscous effects extend over the entire cross section and the **velocity profile no longer changes with increasing x.** The flow is then said to be fully developed, and the distance from the entrance at which this condition is achieved is termed the hydrodynamic entry length, $x_{fd,h}$.

Velocity boundary layer:

$$\mathrm{Re}_D \equiv \frac{\rho u_m D}{\mu} = \frac{u_m D}{\nu}$$

$$\mathrm{Re}_{D,c} \approx 2300$$

For laminar flow ($Re_D \leq 2300$), the hydrodynamic entry length may be obtained from an expression of the form [2]

$$\left(\frac{x_{\mathrm{fd},h}}{D}\right)_{\mathrm{lam}} \approx 0.05\,\mathrm{Re}_D$$

Thermal boundary layer:

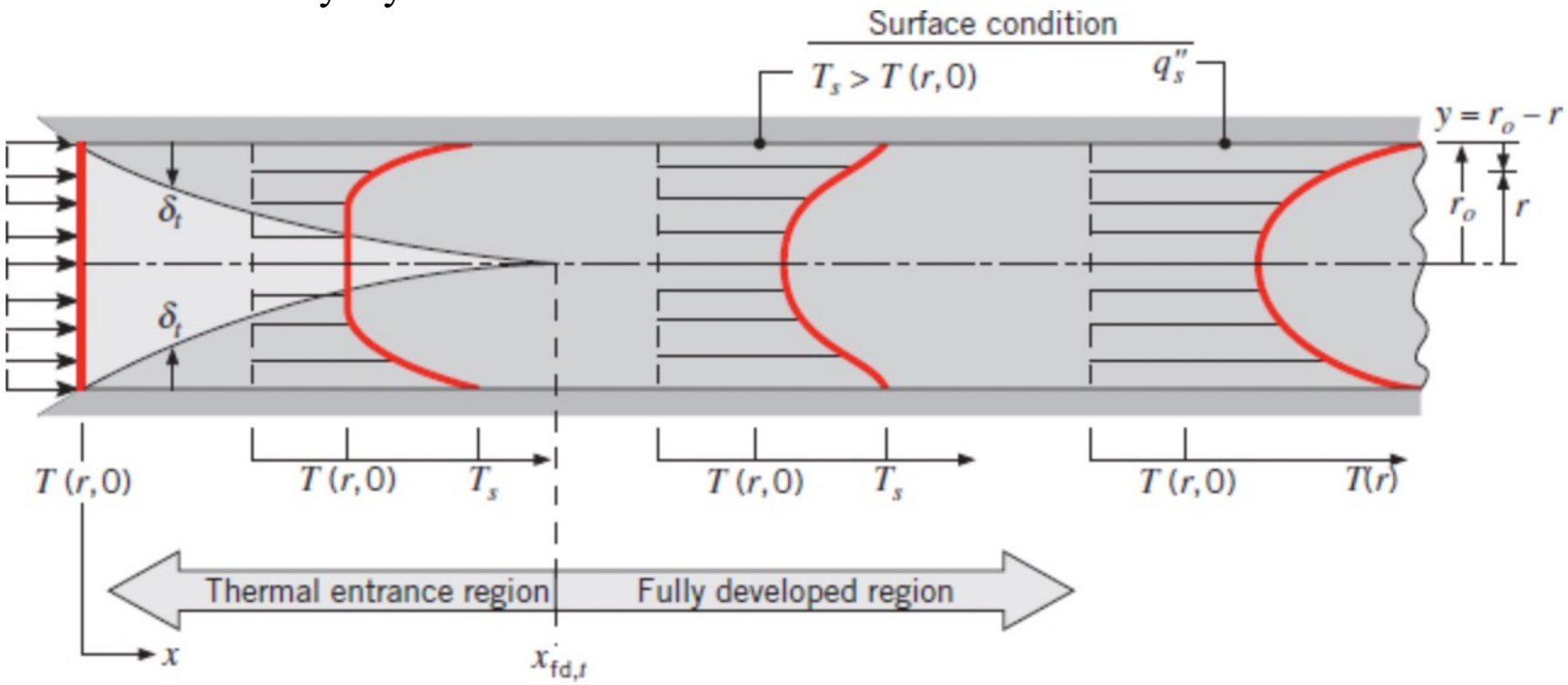

FIGURE 8.4 Thermal boundary layer development in a circular tube with a hot wall.

ength may be expressed as [3]

$$\left(\frac{x_{fd,t}}{D}\right)_{lam} \approx 0.05\,Re_D\,Pr$$